HANS L. SKRIVER

Crystal Structure from One-Electron Theory

ABSTRACT. *We have studied the crystal structures of all the 3d, 4d, and 5d transition metals at zero pressure and temperature by means of the LMTO method and Andersen's force theorem. We find that, although the structural energy differences seem to be overestimated by the theory, the predicted crystal structures are in accord with experiment in all cases except Au. In addition we have investigated the effect of pressure upon the alkali metals (Li, Na, Rb, Cs) and selected lanthanide metals (La, Ce, Lu) and actinide metals (Th, Pa). In these cases the theory gives accurate predictions of the stability of the close-packed structures but is found to be less accurate for open structures such as* α*-U.*

Risø National Laboratory, DK-4000 Roskilde, Denmark

1. Introduction

Many of the characteristic properties of the metallic elements are a consequence of their ability at normal temperature and pressure to form crystals in which the metal atoms are arranged in a regular pattern which repeats itself throughout the interior of the crystal. These crystals are the microscopic building blocks of all the pieces of metal which we encounter around us, and it is therefore of great importance to investigate their basic properties both experimentally and theoretically. The hope is of course that by isolating and understanding the factors that govern the stability of the crystal structures found in nature one may eventually be able to design metals with specified properties.

The crystal structures of solid state materials are established by X-ray diffraction experiments, and the results for the elemental metals are compiled in Fig. 1. It turns out that the variety of crystal structures which the metallic elements take on is limited to essentially the five types shown on Fig. 2, and that four of these five structures are so-called close-packed structures. The term close-packed refers to the fact that the fcc, hcp, dhcp, and Sm-type structures can be derived from stacking hexagonal

0.0 - 0.8											
Li hcp	Be hcp										
Na hcp	Mg hcp	1	2	3.5	5	6	7	8.5	9.5	10	n_d
K bcc	Ca fcc	Sc hcp	Ti hcp	V bcc	Cr bcc	Mn (bcc)	Fe bcc	Co hcp	Ni fcc	Cu fcc	Zn hcp
Rb bcc	Sr fcc	Y hcp	Zr hcp	Nb bcc	Mo bcc	Tc hcp	Ru hcp	Rh fcc	Pd fcc	Ag fcc	Cd hcp
Cs bcc	Ba bcc	Lu hcp	Hf hcp	Ta bcc	W bcc	Re hcp	Os hcp	Ir fcc	Pt fcc	Au fcc	Hg (fcc)
Fr	Ra bcc										

La dhcp	Ce fcc	Pr dhcp	Nd dhcp	Pm dhcp	Sm Sm-t	Eu bcc	Gd hcp	Tb hcp	Dy hcp	Ho hcp	Er hcp	Tm hcp	Yb hcp
Th fcc	Pa bct	U orth.	Np orth.	Pu mon.	Am dhcp	Cm dhcp	Bk dhcp	Cf dhcp	Es	Fm	Md	No	Lr

Fig. 1. Crystal structures of the metallic elements at low temperature.

layers of spheres of equal radii in the closest possible fashion. As a result of this close-packing the coordination number in these four structures is 12, each atom being surrounded by 12 nearest neighbours. The bcc structure is a little less close-packed and has a coordination number of 8, although it is sometimes referred to as having a coordination number of 14 on account of the 6 next nearest neighbours, which are only slightly farther away than the nearest neighbours.

It may be seen from Fig. 1 that the crystal structures of the metallic elements tend to occur in sequences when viewed as functions of atomic number or hydrostatic pressure. The most prominent example of this phenomenon occurs with the d transition metals, where all three transition series, excluding the four magnetic 3d metals, exihibit the same hcp→bcc→hcp→fcc sequence as the d states become progressively filled. A similar sequence is found in the lanthanides where the hcp→Sm-type→dhcp→fcc sequence established as a function of decreasing atomic number may also be realized by subjecting each individual lanthanide metal, except Ce, Eu, and Yb, to hydrostatic pressure. Finally, the alkaline earth metals, together with the divalent rare earths Eu and Yb, are part of a short fcc→bcc sequence which is also realized in Ca, Sr, and Yb under high pressure.

In the present contribution we shall establish the extent to which the systematics outlined above can be explained by means of a state-of-the-art theory for the ground state of the bonding electrons. The theory we apply is a one-electron theory in which each electron is treated as an independent particle moving in the effective potential from all the other electrons and the nuclei, and the only input to the calculations is the atomic number of the metal to be treated. In order to be able to reduce the original many-body problem significantly one has to solve the electronic structure problem self-consistently, and to this end we use the Linear Muffin-Tin Orbital (LMTO) method (Andersen 1975) in conjunction with a scaling principle as outlined by Skriver (1984). The structural energy differences which determine the relative stability of the crystal structures to be studied are in turn obtained from the one-electron states by means of Andersen's force theorem (Mackintosh and Andersen 1980). The whole procedure is quite general and allows us to treat all metals on the same footing.

Fig. 2. Close-packed crystal structures of the elemental metals.

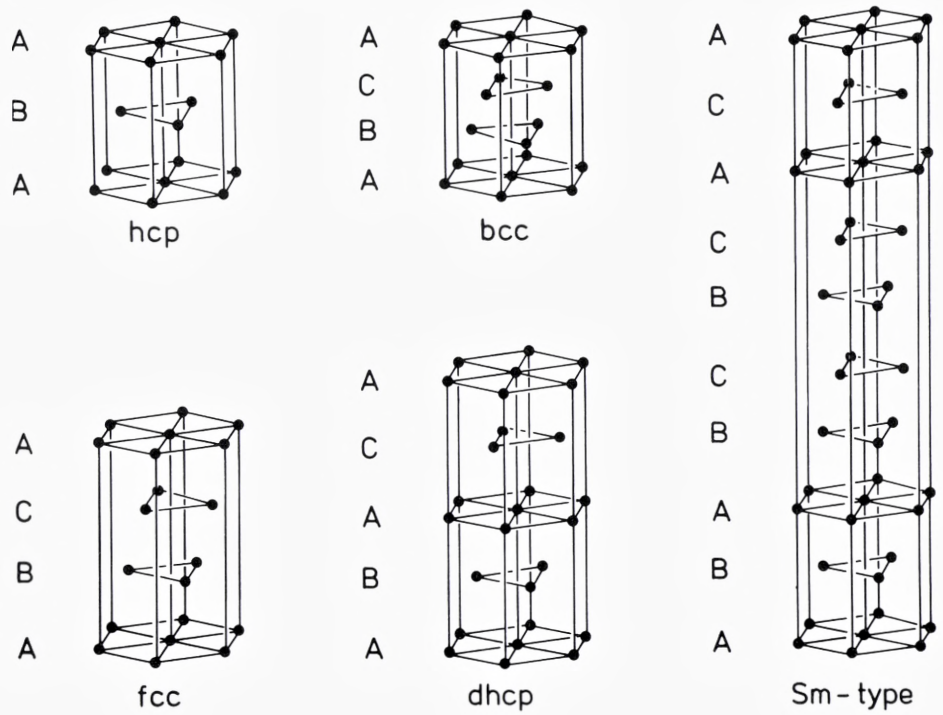

The remainder of the present contribution is organized as follows: In Sect. 1.1 we outline the simplest possible theory of structural stability in terms of the density of electronic states, and in the following section 1.2 we apply this simple theory to state densities obtained by means of canonical band theory. In Sect. 2 we review previous theoretical efforts in the field and compare them with the present approach, the theoretical foundations of which are discussed in Sect. 3. In Sect. 4 we outline an electrostatic correction to the Atomic Sphere Approximation (ASA) which becomes important for structures less close-packed than those shown in Fig. 2. Finally, in Sect. 5 we present the calculated structural energy differences for the alkalis, the alkaline earths, the transition metals, the lanthanides, and the light actinides.

1.1. A simple theory of structural stability

In the main part of the following we shall describe the results of a series of calculations of the relative stability of the crystal structures of some 40 elemental metals. In such a presentation, centred around an account of theoretical results and their relation to experimental observations, it is easy to lose track of the principles upon which the calculations are based. We shall therefore immediately present a simple model which will illustrate these principles and in addition will serve to make more comprehensible the complete calculations to be described later.

According to standard textbooks one may imagine a metal formed in the thought experiment illustrated in Fig. 3 where N initially infinitely separated metal atoms are slowly brought together. Here we shall consider specifically a transition metal in which the important states have d character. As a result of the increasing contact between neighbouring atoms the 5N atomic d states give rise to a band of energies ranging from B which corresponds to bonding between most neighbours to A which corresponds to antibonding between them. The band of energies formed in this way constitutes the energy band of the metal, and it contains all the one-electron states which the conduction electrons may occupy.

The energy gained in the above process is called the cohesive energy, and according to Fig. 3 it is simply the difference between the total atomic energy nE_a and the total band energy $n\bar{E}$, i.e.

$$E_{coh} = n(E_a - \bar{E}) \tag{1}$$

assuming an occupation of n d electrons per atom. In writing down (1) we have furthermore assumed that the d states broaden around the atomic level E_a, that is that the centre C of the d band coincides with E_a.

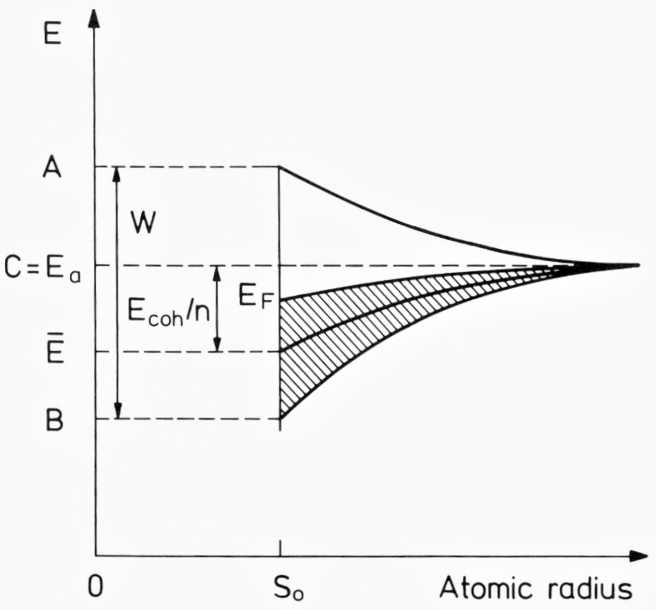

Fig. 3. Formation of the energy band of a metal from an atomic energy E_a. The width is W, the bottom and top B and A, respectively, the Fermi level, i.e. the highest occupied energy E_F, the cohesive energy E_{coh}, and the number of electrons per atom n.

The average energy $\bar{E}$, which corresponds to the centre of gravity of the occupied part of the d band and which enters (1), may be obtained by summing the one-electron energies ε_i between the bottom of the band B and the highest occupied one-electron level E_F, i.e.

$$\bar{E} = n^{-1} \sum_{i}^{occ} \varepsilon_i = n^{-1} \int^{E_F} EN(E)dE \tag{2}$$

where we have introduced the state density function N(E) which describes how the states are distributed in the energy range from B to A.

If we assume that all states within the d band are equally probable the state density will have the rectangular shape shown in Fig. 4a, and the cohesive energy will simply be given by

$$E^r_{coh} = \frac{W}{20} n(10-n) \tag{3}$$

As noted by Friedel (1969) this form clearly exhibits the parabolic variation with the d occupation, cf. Fig. 4, which is also found experimentally (Gschneidner 1969, Friedel and Sayers 1977), especially when proper account is taken of the atomic effects (Brooks and Johansson 1983), and

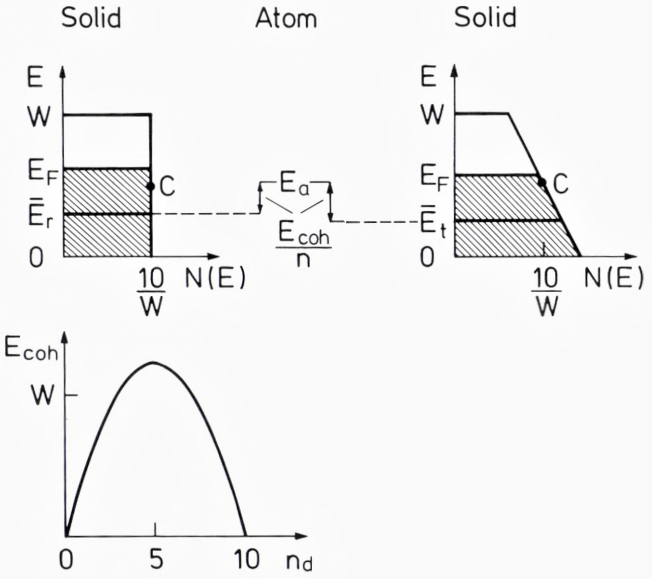

Fig. 4. Rectangular and skew state densities modelling the dependence of the cohesive energy upon crystal structure. The cohesive energy as a function of d occupation n is shown for the rectangular state density at the bottom.

this agreement was taken as confirmation of the assumptions of the model outlined above.

From Eq. (1) and Fig. 4 it is clear that the energy gained in forming a metal from the free atoms depends upon the relative position of the atomic d level E_a and the average band energy $\bar{E}$. The latter depends upon the shape of the state density which in turn depends upon the arrangement of the atoms in the metal crystal, and hence different crystal structures will lead to different cohesive energies.

It follows that the relative stability of all possible crystal structures for a given metal will be determined by the particular shape of the corresponding state densities. We have illustrated this simple result in Fig. 4 from which it is straightforward to see that the crystal structure leading to the skew state density will have a higher cohesive energy and hence be more stable than the structure which leads to the rectangular state density on account of the lowering of $\bar{E}$. Hence, the relative stability of two crystal structures may be estimated simply by comparing the corresponding average band energies $\bar{E}$.

In the complete calculations to be reported later we have applied this simple principle to accurately calculated state densities, and the success with which the results explain the experimental observations may be

taken as a justification of the assumptions underlying the one-electron approach outlined above. As will be explained in Sect. 3 there is however also theoretical justification for such a one-electron approach in the form of the so-called force theorem (Mackintosh and Andersen 1980) which dictates how the band structures and the corresponding state densities of the metals in the different crystal structures should be calculated.

1.2. Structural stability from canonical band theory

The concept of canonical bands (Andersen 1975, Andersen and Jepsen 1977) gives rise to a simple and yet realistic procedure for estimating the relative stability of the close-packed crystal structures which form for instance the transition metal sequence, Fig. 1. According to canonical band theory an unhybridized, pure l band may be obtained from (Andersen and Jepsen 1977, Skriver 1984)

$$E_{li}(\mathbf{k}) = C_l + \frac{1}{\mu_l S^2} \frac{\zeta_{li}^{\mathbf{k}}}{1-\gamma_l \zeta_{li}^{\mathbf{k}}} \tag{4}$$

where $\zeta_{li}^{\mathbf{k}}$ are the canonical bands which depend solely upon the crystal structure, S is the atomic Wigner-Seitz radius, C_l the centre of the l band, μ_l the band mass, and γ_l a distortion parameter. The three potential parameters C_l, μ_l and γ_l depend upon potential and volume but not upon crystal structure.

In a transition metal one may to a good approximation neglect all but the d bands. Since furthermore γ_d is small, one has the following potential-, i.e. atomic number-, independent estimate of the band contribution to the cohesive energy E_{coh}

$$\begin{aligned} \mu_d S^2 E_{coh} &= -\mu_d S^2 \int^{E_F} (E - C_d)\, N_d(E)\, dE \\ &= -\int^{\zeta_d(n_d)} \zeta_d\, \tilde{N}_d(\zeta_d)\, d\zeta_d \end{aligned} \tag{5}$$

in terms of the first-order moment of the canonical state density $\tilde{N}_d$. Andersen et al. (1977) have evaluated (5) as a function of d occupation number n_d and found the expected parabolic behaviour (Friedel 1969) which may also be obtained directly if $N_d(E)$ is approximated by a rectangular state density as explained in the introduction.

Since the centre C_d and the band mass μ_d are independent of crystal structure, the first-order moment (5) may be used to estimate the structural energy differences according to Eq. (9). The result shown in Fig. 5 is identical to that of Andersen et al. (1977) and similar to the one

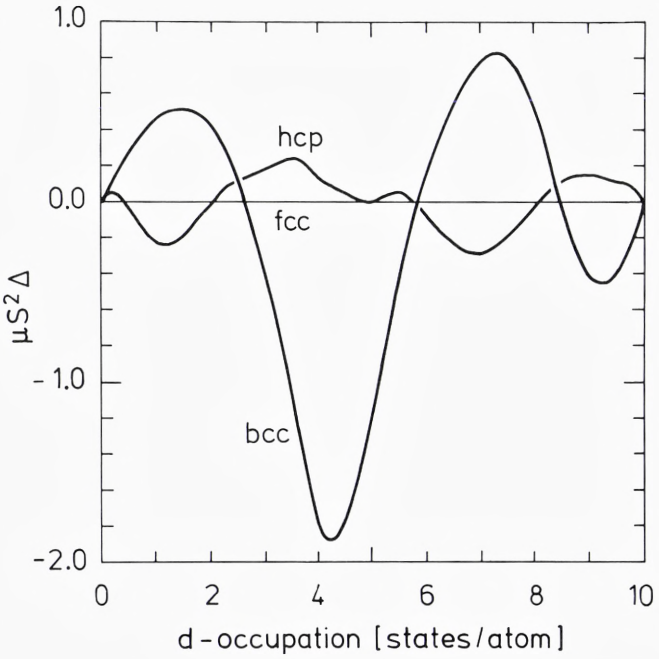

Fig. 5. Structural energy differences obtained from canonical d bands by means of Eq. (5) as functions of the calculated canonical d occupation.

obtained by Pettifor (1970). It accounts qualitatively for the crystal structures of the non-magnetic transition metals, Fig. 1, in the beginning of the series but fails to predict the fcc structure at high d occupations. This failure is attributed either to a failure of the force relation (Mackintosh and Andersen 1980) or to hard-core effects (Pettifor 1970, 1972, 1977) omitted i Eq. (5).

The lanthanide metals are found to have d occupation numbers varying almost linearly with atomic number from 1.99 in La to 1.45 in Lu (Skriver 1983) or from 2.5 to 2.0 if hybridization is neglected (Duthie and Pettifor 1977). Furthermore, their crystal structures are as closely packed as are those of the d transition metals and hence their structural energy differences may be estimated by Eq. (5). The results shown in Fig. 6 are qualitatively similar to but on the average a factor 1.7 smaller than those obtained by Duthie and Pettifor (1977). In this comparison one may take the d-band width to be approximately $25/\mu_d S^2$ in order to bring their Fig. 2 onto the scale of Fig. 6. The results in Fig. 6 account qualitatively for the hcp→Sm-type→dhcp sequence found experimentally in going from Lu to La and more importantly perhaps, since the d occupation for the lanthanides is calculated to increase with pressure and

decrease with atomic number, they also explain that part of the same sequence is realized when a particular lanthanide metal is subjected to pressure. It therefore follows that the d occupation number, which is essentially a measure of the relative position of the s and d bands, may be used to rationalize the structure of the generalized phase diagram for the lanthanides constructed by Johansson and Rosengren (1975).

At the present stage one should realize that the results obtained by canonical band theory and shown in Figs. 5 and 6 are only qualitative. Indeed, if one considers Fig. 7 where the canonical estimates are compared with experimental crystal structures, one finds that the canonical theory in several cases does not predict the correct crystal structure independently of whether one uses the self-consistent d occupation num-

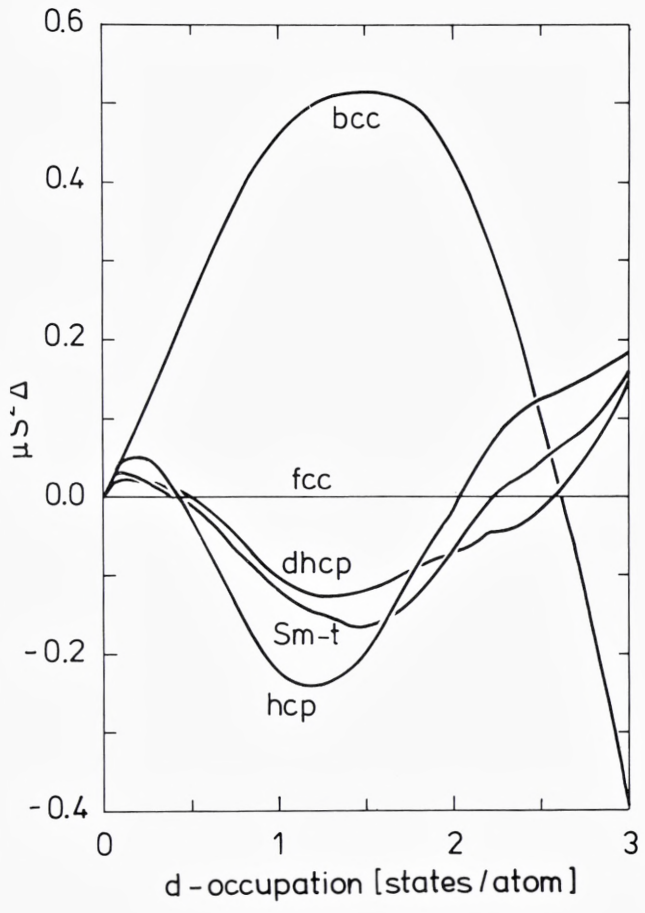

Fig. 6. Structural energy differences obtained from canonical d bands by means of Eq. (5) in the d occupation number range appropriate to the lanthanide crystal structure sequence.

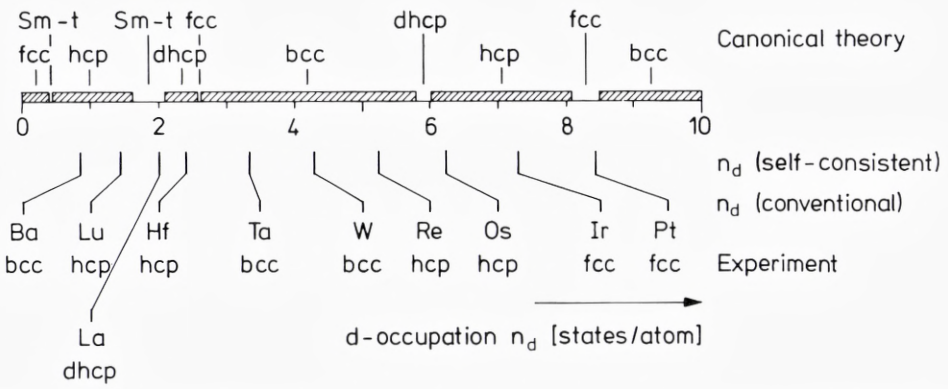

Fig. 7. Canonical estimate of the most stable close-packed crystal structure as a function of the calculated d occupation number compiled from Figs. 2 & 3, horizontal bars. Below are given two estimates of the actual d occupation numbers of the 5d metals together with the experimentally observed crystal structures.

bers or those obtained conventionally by nonlinear interpolation along a row in the periodic table (see Fig. 1). La, Re, and Ir, for instance, are examples of incorrect predictions, but here one may argue that the correct crystal structure is nearby and hence the failure of the theory may be considered less important. Ba is another example and in this case there is no nearby bcc structure. However, in Ba the d occupation number is only a fraction of the total number of electrons and hence a theory based solely upon unhybridized d bands is probably inapplicable. The most important failure is connected with the d occupation range from 1.6 to 2.6 [states/atom]. According to Fig. 7, La, Pr, Nd, and Pm should incorrectly form in the Sm-type structure while Ti, Zr, and Hf are expected to be part of the lanthanide sequence. Instead, the latter three metals form in the hcp structure which is the least stable among those considered in the d occupation range above 2 [states/atom].

It may be concluded that the simple estimate of structural energy differences obtained by means of the first-order moments of the canonical state densities is of limited value as a predictive tool. It is, however, of sufficient physical significance to warrant a study of the crystal structures of metals using a more accurate one-electron theory, and to be used in the interpretation of the results of such a study.

2. Theoretical approaches to structural stability

The most prominent crystal structure sequence in the periodic table is the hcp→bcc→hcp→fcc sequence found among the d transition metals, see Fig. 1. Qualitative explanations of this trend have been given by Brewer (1967) in terms of Engel correlations between the valence sp electrons and by Kaufman and Bernstein (1970) in terms of semi-empirical thermodynamic calculations of phase diagrams, whereas Deegan (1968), Dalton and Deegan (1969), and Ducastelle and Cyrot-Lackmann (1971) have attempted more quantitative approaches based upon one-electron theory.

Deegan (1968) and Dalton and Deegan (1969) showed that the stability of the bcc phase for nearly half-filled d shells might be explained by differences in the sum of one-electron band structure energies, and they pointed to the special double-peak structure of a bcc state density as responsible for this stability. Later, Pettifor (1970, 1972) extended the work of Dalton and Deegan and showed that the entire crystal structure sequence of the transition metals could be accounted for by a one-electron approach. In his calculations Pettifor (1977) found no evidence for the Brewer-Engel correlation (Brewer 1967), which relates crystal structure stability to the sp occupation numbers, and instead he related the hcp→bcc→hcp→fcc sequence to the change in d occupation which takes place across a transition series. This latter viewpoint has proven to be very fruitful in that it may be used as a simple »one-parameter theory« which in many cases provides remarkably good estimates of structural stabilities also for non-transition metals such as the alkaline earths (Skriver 1982).

The crystal structures of the trivalent lanthanides, i.e. Pr through Lu except Eu and Yb, exhibit such regularity, as functions of atomic number, pressure, and temperature, that Johansson and Rosengren (1975) were able to construct a single generalized phase diagram for these metals. In this case the crystal structures observed under ambient conditions, (see e.g., Beaudry and Gschneidner 1978) are found to be part of the sequence hcp→Sm-type→dhcp→fcc→fcc' established by high-pressure experiments (Jayaraman and Sherwood 1964, Piermarini and Weir 1964, Jayaraman 1965, McWhan and Stevens 1965, 1967, Liu et al. 1973, Liu 1975, Nakaue 1978) and alloying (Koch 1970). Here fcc' refers to the recently discovered distorted fcc structure (Grosshans et al. 1981). The lanthanide sequence is also found in Y (Vohra et al. 1981) where there are no occupied f states and in the heavier actinide (Stephens et al. 1968,

Akella et al. 1979, 1980, Roof et al. 1980, Roof 1982, Benedict et al. 1984) at pressures where the 5f states are still localized. Qualitative explanations of the hcp→Sm-type→dhcp→fcc sequence have been attempted in terms of pseudopotential theory by Hodges (1967) and in terms of a 4f contribution to the bonding by Gschneidner and Valletta (1968), while Duthie and Pettifor (1977) gave a quantitative explanation in terms of one-electron theory.

Duthie and Pettifor (1977) showed that the lanthanide crystal structure sequence could be explained by differences in the total one-electron band structure energies, and they found a strong correlation between crystal structure and d-occupation number. Hence it appears that the lanthanide metals, as far as their crystal structures are concerned, behave as ordinary 5d transition metals with a d occupation ranging from approximately 2.0 in La to 1.5 in Lu. This result is very appealing because there is a one-to-one correspondence between the calculated d-occupation number and the single f parameter used by Johansson and Rosengren (1975) and Johansson (1978) to rationalize the lanthanide crystal structure sequence, and because it is immediately possible to understand the behaviour of Y (Vohra et al. 1981) and the heavy actinides (Stephens et al. 1968, Akella et al. 1979, 1980, Roof et al. 1980, Roof 1982, Benedict et al. 1984) within the same framework.

At first sight it may seem surprising that the crystal structures of so many metals can be explained on the basis of differences in the total one-electron band structure energies alone, since the total electronic energy, apart from the one-electron term, has contributions also from double counting and exchange-correlation. However, it has recently been shown (Andersen et al., 1979, Mackintosh and Andersen 1980, see also page 119 of Heine 1980) that, provided the one-electron *potential* is kept frozen upon a displacement of the atoms, the corresponding changes in the double counting and exchange-correlation terms cancel to first order in the appropriate local electron density, and hence the difference in the sum of the one-electron energies, obtained by means of the frozen, i.e. not self-consistently relaxed, potential, will give an accurate estimate of the corresponding self-consistent change in the total electronic energy. It is exactly this cancellation, which also leads to the so-called pressure expression (Nieminen and Hodges 1976, Pettifor 1976) and to the more general force relation derived by Andersen (see Mackintosh and Andersen 1980), that in turn justifies the simple band structure approach taken for instance by Pettifor (1970, 1972, 1977).

In their work Pettifor (1970, 1972, 1977) and Duthie and Pettifor

(1977) focused their attention on the contribution to the total energy from the d bands and either neglected hybridization with the sp bands entirely or included hybridization appropriate to some average element. Hence their picture is essentially a canonical one (cf. Sect. 1.2) in which the energy band structures depend only upon crystal structure and not upon band-filling. It is obvious that such a picture, although adequate for the d transition metals, will fail in cases where states of non d character are as or more important than the d states, as they are for instance in the alkali, the alkaline earth and light actinide metals. Fortunately, the force theorem is not restricted to the canonical approximation and it has recently been used in theoretical investigations of crystal structures in the third row metals (Moriarty and McMahan 1982, McMahan and Moriarty 1983) the alkaline earth metals (Skriver 1982), and in Cs above the s-d transition (McMahan 1984).

In the present work we go beyond the canonical approximation and use the force theorem (Mackintosh and Andersen 1980) to calculate the structural energy differences for all the 3d, 4d, and 5d transition metals at zero pressure and temperature. In addition we investigate the effect of hydrostatic pressure upon the crystal structures of alkali, alkaline earth, lanthanide and actinide metals.

Traditionally the non-transition metals, e.g. alkali and alkaline earth metals, have been treated by means of pseudopotential theory, and the crystal structures predicted from this approach are generally in good agreement with experiment (Animalu 1967, Heine and Weaire 1970, Moriarty 1973, 1982, Hafner and Heine 1983, Young and Ross 1984). It has, however, not been straightforward to generalize the pseudopotential method to treat narrow d band materials, and to do so one has had to add localized orbitals to the plane-wave basis (Zunger and Cohen 1979). Thus the d band in K is described by the d component of plane-waves while that of Cu is described by additional d orbitals, which is somewhat inconsistent with the smooth lowering of the 3d band through the series K, Ca, Sc, ..., Cu. The method has, however, proved to be very accurate.

The present approach, based upon the Linear Muffin-Tin Orbital (LMTO) method (Andersen 1975), has the advantage of employing the same type of basis functions for all the elements thus leading to a conceptually consistent description of trends throughout the periodic table. In addition, the LMTO method is extremely efficient on a computer requiring only the solution of an eigenvalue problem of 9×9 (or 16×16 if f states are included) per atom at each point in reciprocal space. Since we

are mainly interested in trends, we have neglected the nonspherical contributions to the charge density, which may explain what seems to be a systematic overestimate of the calculated structural energy differences. We have furthermore neglected a structure-dependent electrostatic interaction between atomic spheres except in the few cases where it contributes significantly to the energy differences.

3. One-electron theory of structural stability

At low temperatures the crystal structure of a metal is determined by the total electronic energy U in addition to a small contribution from the zero-point motion*, which we shall neglect. Hence, if one wants to determine the stability of some crystal structure, say bcc, against some reference structure, which we shall take to be the close-packed fcc structure, one may calculate the total energy of both phases and form the structural energy difference

$$\Delta_{\text{bcc-fcc}} = U_{\text{bcc}} - U_{\text{fcc}} \tag{6}$$

where the total energy according to the local density approximation (Kohn and Sham 1965) may be written as the sum over occupied states of the one-electron energies ε_i corrected for double counting, plus electrostatic terms (see e.g., sections 13 and 15 of Heine 1980 or sections 7.2 and 7.3 of Skriver 1984), i.e.

$$U = \sum_{i}^{\text{occ}} \varepsilon_i - \text{double counting} + \text{electrostatic} \tag{7}$$

If the difference (6) is negative the bcc structure will be stable against fcc.

The total energy for say a 4d metal is of the order of 10^4 [Ry] mainly because of the contributions from the low-lying core levels while typical structural energy differences are of the order of 10^{-3} [Ry]. Hence, extreme accuracy is needed in order to use (6) directly, and one would like to have a numerically more satisfactory procedure. The force theorem (Mackintosh and Andersen 1980) gives rise to such a procedure, but more importantly perhaps it casts the problem of finding stable crystal

* The zero-point energy is proportional to the Debye temperature i.e. $E_o = (9/8)\, k_B\, \Theta_D$. Typically Θ_D varies by 1-10 [K] between different structures of the same metal (see Gschneidner 1964) and hence the ΔE_o to be added to (6) is of the order of 0.01-0.1 [mRy] which in most cases will be too small to affect the structural stabilities.

structures into a form where the significant contribution comes from the one-electron valence energies and not from double counting nor from the deep core-levels.

The force theorem dictates that we adopt the following procedure: For a given metal at a given atomic volume one must solve the energy-band problem self-consistently assuming the reference crystal structure. To this end we use the LMTO method (Andersen 1975) within the Atomic Sphere Approximation (ASA) including the combined correction to the ASA (Andersen 1975). In addition we take account of the relativistic effects, except spin-orbit coupling which we neglect, include exchange-correlation in the form given by von Barth and Hedin (1972), and freeze the appropriate cores. This part of the calculations is described in detail by Skriver (1984). We have now minimized the energy functional $U\{n\}$ with respect to changes in the electron density n and obtained the ground state density n^{sc}_{fcc}. Because of the stationary properties of U one may obtain, for instance, U_{bcc} from a trial charge-density n^{tr}_{bcc} constructed by positioning the self-consistent fcc atomic-sphere *potentials* in a bcc geometry, solving the one-electron Schrödinger equation, and populating the lowest-lying one-electron states. Hence,

$$\Delta_{bcc-fcc} = U_{bcc}\{n^{tr}_{bcc}\} - U_{fcc}\{n^{sc}_{fcc}\} \tag{8}$$

where the errors relative to (6) are of second order in $n^{tr}_{bcc} - n^{sc}_{bcc}$. Now, the use of a *frozen,* i.e. not self-consistently relaxed, *potential* to generate n^{tr}_{bcc} ensures that the chemical shifts in the core levels drop out of Eq. (8) and also that the double-counting terms cancel. Hence, the core level energies and the double-counting terms may be neglected entirely in Eq. (7) leaving only the valence one-electron energies and the electrostatic terms to be considered. The fact that the freezing of the potential leads to such a computationally simple and conceptually important result was already noted by Pettifor (1976) in his derivation of the pressure expression.

Within the atomic sphere approximation (Andersen 1975) the atomic Wigner-Seitz sphere of an elemental metal is neutral and there is therefore no electrostatic interaction between the spheres. Hence the electrostatic terms in Eq. (7) vanish and the structural energy difference (8) may be obtained from

$$\Delta_{bcc-fcc} = \int^{E_F} E\, N_{bcc}(E)\, dE - \int^{E_F} E\, N_{fcc}(E)\, dE \tag{9}B$$

where N(E) is the one-electron state density. Furthermore, the ASA allows a separation of the potential- and crystal-structure-dependent

parts of the energy band problem (Andersen 1975, Andersen and Jepsen 1977, Skriver 1984). Hence, all that is required at a given atomic volume, in addition to the self-consistent fcc calculation, is to calculate the energy bands of the relevant crystal structures with the use of the self-consistent fcc potential parameters, evaluate the sums of the one-electron energies, and subtract according to Eq. (9). This procedure is quite general, treats all s, p, d, and f electrons on the same footing, and may be applied to all metals in the periodic table.

4. Madelung correction to the ASA

The errors of neglecting the structure-dependent electrostatic terms in (7) may be estimated by means of what has been called either the Muffin-Tin (Glötzel and Andersen, unpublished) or Ewald (Esposito et al. 1980) correction to the ASA. To derive this correction one observes that the electrostatic energy per ion of a lattice of point ions of charge $q_s|e|$ embedded in a negative neutralizing uniform charge density is given by the well-known Madelung expression

$$U_M = -1/2(q_s|e|)^2 \frac{\alpha_M}{S} \tag{10}$$

where α_M is the lattice Madelung constant and S the atomic Wigner-Seitz radius. In the ASA this expression is approximated by the energy of an ion embedded in a single neutralizing atomic sphere, whereby $\alpha_M(\text{ASA}) = 1.8$. The correction is therefore

$$\Delta U_M = 1/2(q_s|e|)^2 \frac{1.8-\alpha_M}{S} \tag{11}$$

In a Muffin-Tin model the effective charge $q_s|e|$ is the charge density in the interstitial region between the Muffin-Tin spheres times the volume of the unit cell. In the ASA this becomes

Tabel 1. Madelung constant to be used in Eq. (11).

	α_M	$1.8-\alpha_M$	$(1.8-\alpha_M)-(\ )_{fcc}$
fcc	1.79174723	$8.253\ 10^{-3}$	
bcc	1.79185851	$8.142\ 10^{-3}$	$-\ 0.111\ 10^{-3}$
hcp	1.79167624	$8.324\ 10^{-3}$	$0.071\ 10^{-3}$
α-U⋆)	1.78418298	$15.817\ 10^{-3}$	$7.564\ 10^{-3}$

⋆) b/a = 1.964, c/a = 1.709, y = 0.1

$$q_s|e| = \frac{4\pi}{3} S^3 n(S) |e| \tag{12}$$

where n(S) is the electron density at the atomic radius.

For close-packed crystal structures α_M is approximately 1.8, see Table 1, and hence the correction (11) is smallest in these. Typically q_s^2/S lies in the range from 0.5 to 5 [a.u.] so that the Madelung correction for the bcc and hcp structures relative to the fcc structure lies in the range 0.05 to 0.5 [mRy].

5. Structural stability from LMTO band calculations

In the following we shall present structural energy differences for most metallic elements to the left of and including the noble metals as obtained by means of the procedure described in Sect. 3. The results will be valid only at low temperature and at atmospheric pressure, strictly T = 0[K] and P = 0 [GPa], except in a few important cases where structural stability has been followed as a function of pressure.

5.1. The alkali metals

The calculated structural energy differences for alkali metals at equilibrium are almost two orders of magnitude smaller than those of, for instance, the alkaline earth metals. To judge the accuracy of our approach we have therefore studied these differences as functions of pressure as shown in Fig. 8 from equilibrium down to a compression of 2.5. The results in Fig. 8 include the Madelung correction (11) which turns out to be crucial in the comparison with recent pseudopotential and LMTO results (Moriarty 1982, Moriarty and McMahan 1982, McMahan and Moriarty 1983).

From Fig. 8 it is expected that the heavy alkalis at low temperature and pressure should form in the bcc structure while Li should be hcp. Experimentally it is known (Donohue 1975, Young 1975) that all five alkali metals at room temperature form in the bcc structure, and that they remain in this structure down to 5 [K] except Na which below 51 [K] transforms into the hcp structure and Li which at low temperature exhibits both an hcp and an fcc phase. Hence, except for Na the low pressure structures are correctly predicted.

Recently, Moriarty (1982) successfully estimated the structural stability for some 20 non-transition metals by means of his Generalized Pseudopotential Theory (GPT). He found incorrectly (see his Table VIII)

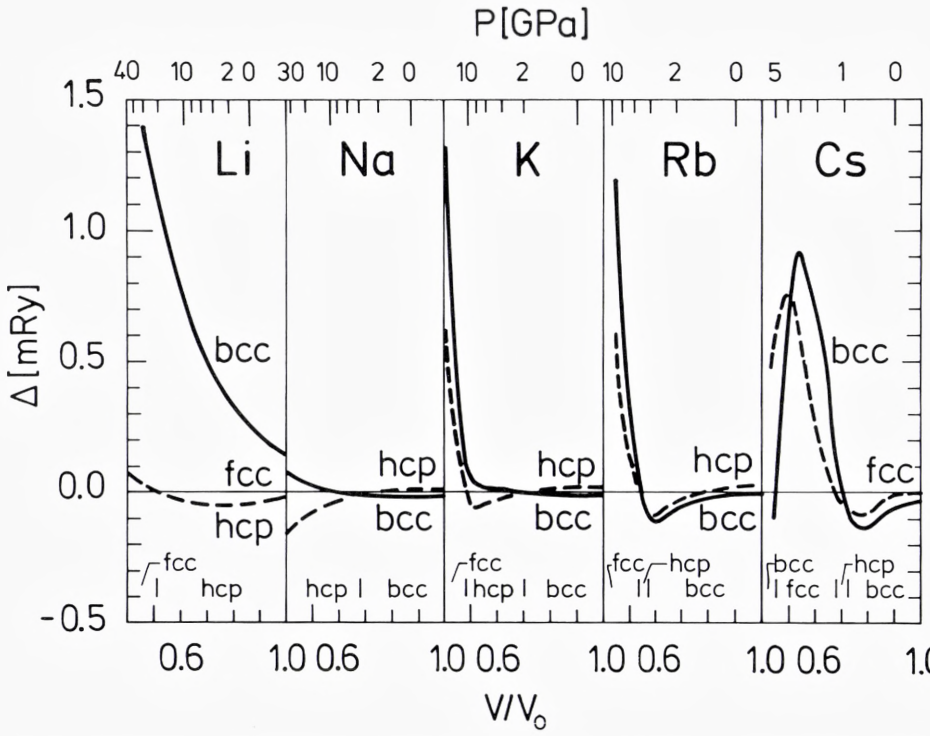

Fig. 8. Structural energy differences for the 5 alkali metals as functions of the relative volume V/V_o. At the top is given the calculated LMTO pressure P. The calculations included s, p, and d orbitals and the Madelung correction Eq. (11).

that all the alkali metals at P = 0 and T = 0 should form in the hcp structure, but pointed out that at a slight compression the experimentally observed bcc structure would be stable in the heavy alkalies K, Rb, and Cs. A similar problem is encountered in another recent pseudopotential study (Young and Ross 1984) where the structures of Li and K at low temperature and pressure are predicted in agreement with experiment but where Na is expected to be fcc. On the other hand, in view of the extremely small energies involved, see Fig. 8, it is not surprising that the prediction of the low-pressure part of the alkali phase diagrams is a severe test of any calculation.

In their work on the third-row metals McMahan and Moriarty (1983) compared structural energy differences obtained by means of the LMTO and GPT methods and found excellent qualitative agreement except for Na. If we compare our Na results in Fig. 8 with their Fig. 1 we find

somewhat surprisingly that our calculations are in closer agreement with their GPT than with their LMTO results. There are several reasons for the differences between the two LMTO calculations. Firstly, we have included the Madelung correction (11) without which the calculated bcc curve is entirely above and the hcp curve entirely below the fcc, in qualititative agreement with their LMTO results. Secondly, we have sampled the Brillouin zone on a finer mesh, i.e. 916, 819, and 448 points in the irreducible wedge for fcc, bcc, and hcp, respectively, and finally, we have improved the convergence of the reciprocal lattice sums in the expression for the combined correction terms (Andersen 1975) whereby the numerical errors in the structural energy differences for Na are below 0.01 mRy. As a result it appears that in the case of closely packed crystal structures the LMTO method including the Madelung correction (11) has an accuracy comparable to that attained by pseudopotential theory.

Owing to the inclusion of only three crystal structures in Fig. 8, Cs is incorrectly calculated to transform into the bcc structure at a compression of 2.2. However, in a recent study of Cs above the s-d transition, i.e. beyond the pressure range of the present work, McMahan (1984) found that Cs had transformed into the Cs IV structure before the bcc structure became more stable than fcc, in agreement with high pressure experiments (Takemura et al. 1981, 1982).

5.2. The alkali metals at moderate compression

According to Fig. 8 all the alkali metals should at low temperature be part of the same crystal structure sequence bcc→hcp→fcc, and one would anticipate that these transitions are driven by the pressure-induced lowering of initially unoccupied d states through the Fermi level, whereby electrons are gradually transferred from the s into the d band. If one plots the calculated crystal structures as functions of d occupation number as in Fig. 9 it is seen that only in the heavy alkalis K, Rb, and Cs is this mechanism at work while the transitions in Li and Na at least below 35 [GPa] have a different origin.

The experimental situation at room temperature has recently been summarized as follows (Takemura and Syassen 1983, Olijnyk and Holzapfel 1983). Li exhibits a bcc→fcc transition at 6.9 [GPa] (Olinger and Shaner 1983) while Na remains in the bcc structure up to at least 30 [GPa] (Alexandrov et al. 1982) which substantiates the notion that the s-d transition is unimportant in these two metals. The heavy alkalis all exhibit a bcc→fcc transition [K (Takemura and Syassen 1983, Olijnyk and Holzapfel 1983), Rb (Takemura and Syassen 1982), Cs (Hall et al.

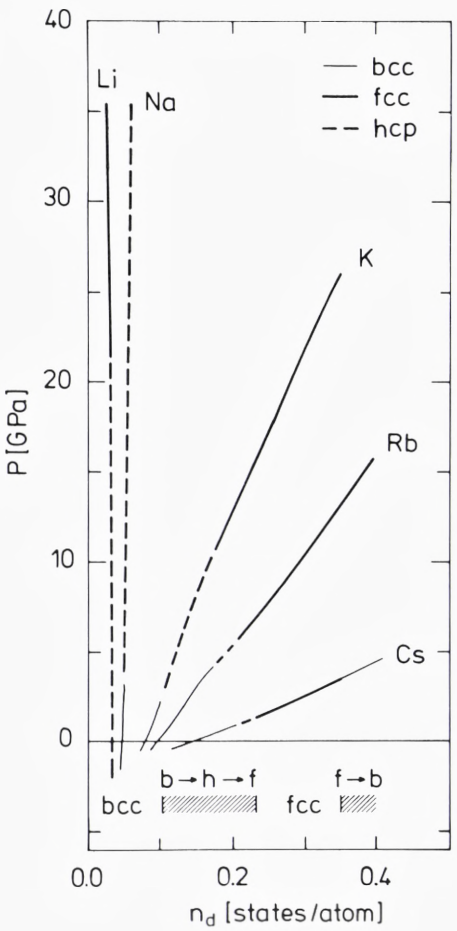

Fig. 9. Calculated crystal structures for the alkali metals as functions of the LMTO pressure and d occupation number.

1964)] before they transform into more complex structures of which only the so-called Cs IV has been solved so far (Takemura et al. 1982).

To our knowledge there are no low-temperature high-pressure experiments which could substantiate the existence of the predicted bcc→hcp→fcc sequence, where according to Figs. 8 and 9 the hcp phase at least in K should be stable over an appreciable pressure range. However, in view of the fact that temperature at atmospheric pressure stabilizes the bcc phase to the extent that all the alkali metals are bcc above 100 K it is reasonable to assume that the intermediate hcp phase, which is only marginally stable, is also suppressed at higher temperatures. Thus, in a high-pressure experiment at room temperature one would see a direct bcc→fcc transition, as indeed one has observed (Hall et al. 1964, Take-

mura and Syassen 1982, 1983, Olijnyk and Holzapfel 1983). If the hcp phase is suppressed the best estimate of the room temperature bcc→fcc transition pressure is the critical pressure for the low-temperature hcp→fcc transition (cf. Fig. 8). We find the transition pressures to be 11, 5.5, and 1.4 [GPa] for K, Rb, and Cs, respectively, which should be compared to the experimental values of 11, 7, and 2.2 [GPa] listed in the references cited above.

Independent of whether the intermediate hcp phase exists or not, the high-pressure fcc phase in K, Rb, and Cs is much more stable than the initial bcc phase, see Fig. 8. Bardeen (1938) suggested already in 1938 that the transition observed at 2 [GPa] in Cs was from the normal bcc to an fcc phase and that it resulted from the non-electrostatic interaction energy of the ions, the important term being the Born-Mayer (Born and Mayer 1932) repulsion between the ion cores. Here we shall show that the fcc phase in the heavy alkalies owes its stability directly to the pressure-induced s-d transition which is also shown to be behind, for instance, the isostructural fcc-fcc transition in Cs (Glötzel and McMahan 1979).

In Fig. 10 we compare the important parts of the fcc and bcc band-structures of Cs at the zero-pressure volume, V_o, and at the volume where the fcc phase becomes more stable than the initial bcc phase. The four band structures may be characterized as nearly free-electron and s-like below the Fermi level E_F and d-like above E_F. Typical d states have symmetry labels such as Γ_{12}, $\Gamma_{25'}$, H_{12}, and X_3, and they are seen to approach the Fermi level under compression. At $V = V_o$ the fcc and bcc band-structures are found to be extremely similar in the range below E_F which is important in the sums over occupied states in Eq. (9): They are both parabola shaped and »touch« E_F at a single symmetry point, L_1 for fcc and N_1 for bcc. As a result, the sum of the one-electron band-structure energies are almost equal and the main contribution to the stability of the bcc phase comes from the electrostatic Madelung term (11) which is negative, see Table 1.

At $V = 0.7\ V_o$ hybridization with the descending d band has moved the X_1 and neighbouring levels below E_F thereby lowering the energy in the fcc phase with respect to that in the bcc phase to the extent that the Madelung term is overcome and the structural energy difference is zero. Under further compression the X_1 level continues to descend and the fcc phase becomes increasingly stable, see Fig. 11. This trend is eventually broken because the maximum in the $\Gamma_1\Delta_1X_1$ band moves away from X and because the X_3 level drops below the Fermi level. Both effects de-

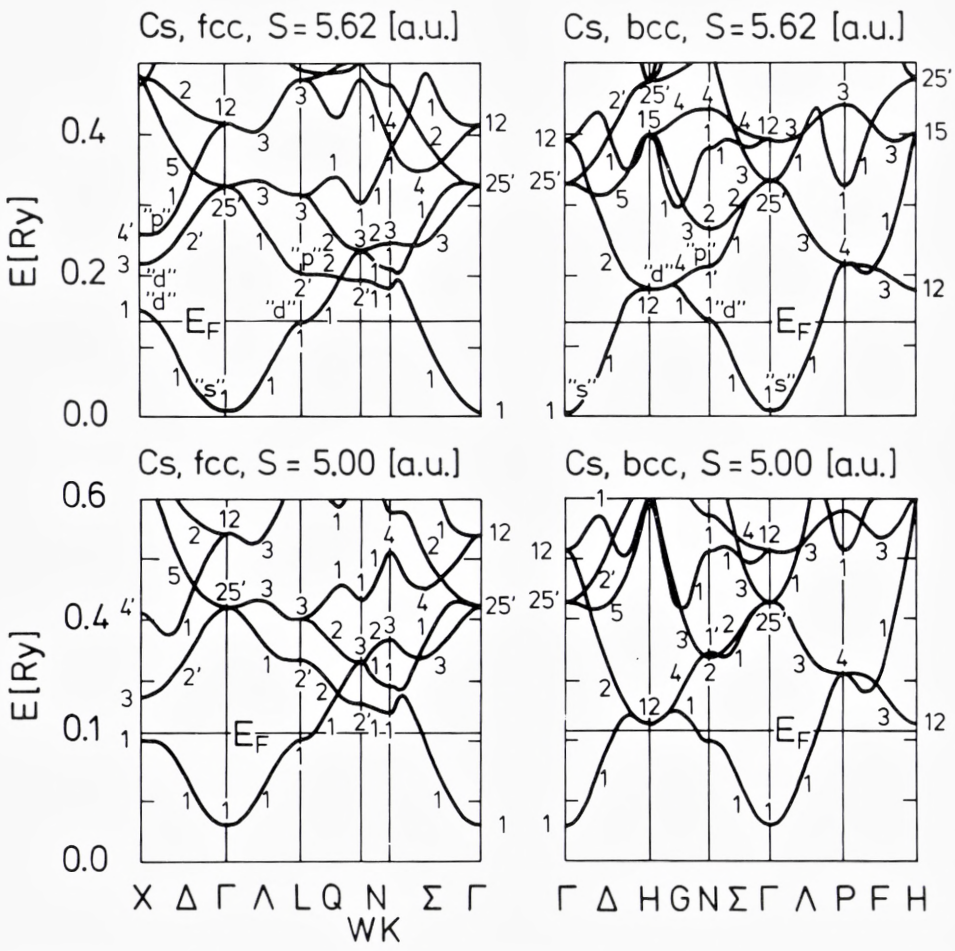

Fig. 10. Energy band structures for Cs at equilibrium, S = 5.62 [a.u.], and at a compressed volume, S = 5.0 [a.u.]. Conventional symmetry labels are given and the dominant s, p or d character is indicated at a few selected energy levels.

stabilize the fcc structure and subsequently Cs transforms into the Cs IV phase. We shall not discuss this development here but refer to the experimental work of Takemura et al. (1982) and the theoretical treatment of McMahan (1984).

The presence of a gap at X (see Fig. 10) near the Fermi level in the compressed fcc phase which has no counterpart in bcc phase (nor in the hcp phase) stabilizes the fcc phase over the bcc in exactly the manner discussed by Jones in his classical work on the phase boundaries in binary

alloys (Mott and Jones 1936, Jones 1937). The electron states below the gap have their one-electron band-energies lowered and are more densely populated than their free-electron or, here, bcc counterparts. The way the fcc phase is stabilized in Cs under pressure is shown in Fig. 11 where one notes that the stabilization occurs gradually from the point where the X_1 level crosses E_F. Hence, although the fcc phase eventually becomes more stable than the bcc phase because of the presence of the band gap at X, there is no direct relation between the volume ($V = 0.70\ V_o$) where the phase transition occurs and the volume ($V = 0.82\ V_o$) where the van Hove singularity connected with the X_1 level moves through the Fermi level. This delayed action is characteristic of many electronically driven transitions.

In the discussion of the stability of the fcc phase we have considered only Cs for simplicity, but examination of the band structures for K and Rb shows that the above picture applies equally well to these two metals although there are quantitative differences between K, Rb, and Cs caused by the fact that the zero-pressure position of the initially unoc-

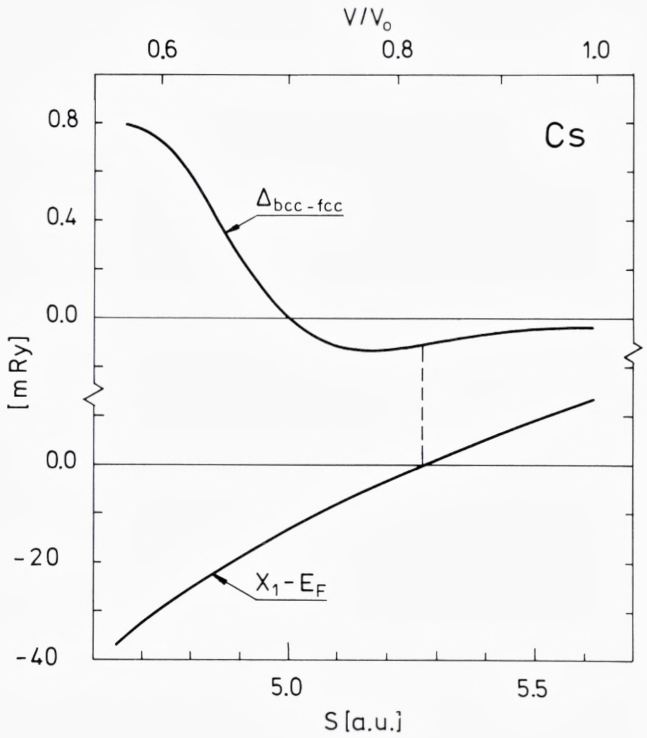

Fig. 11. Structural energy difference $\Delta_{bcc\text{-}fcc}$ for Cs, upper panel, and the position relative to the Fermi level, E_F, of the bottom of the gap at X in the fcc structure, lower panel, as functions of atomic radius, S, or relative volume V/V_o. $V = (4\pi/3)S^3$.

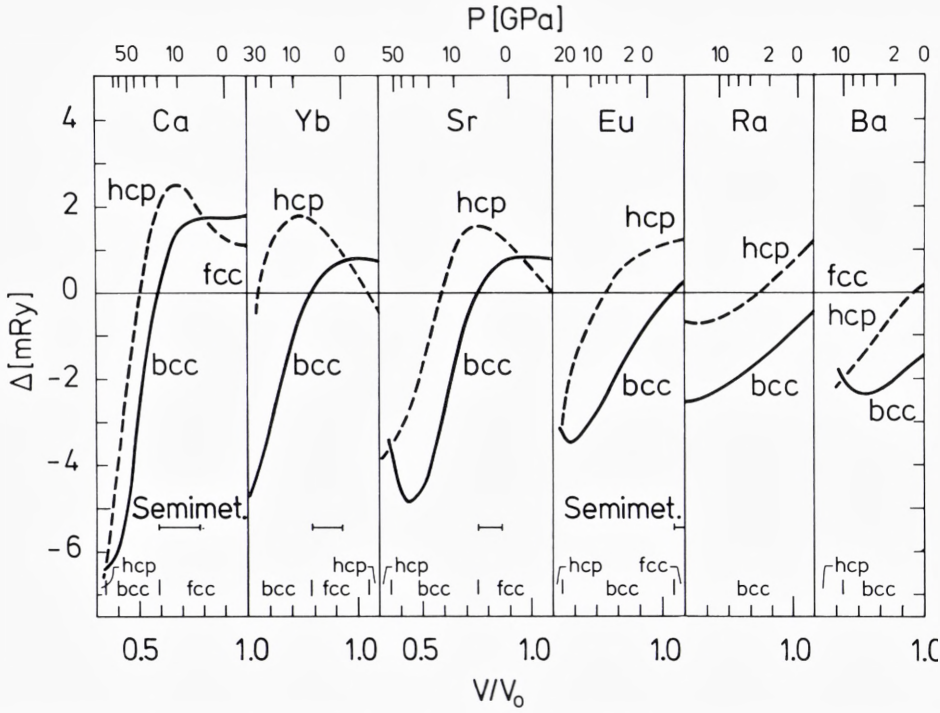

Fig. 12. Structural energy differences for the alkaline earth metals and the two divalent rare earths Eu and Yb as functions of relative volume V/V_0 and LMTO pressure P. The volume range over which the elements are calculated to be semimetallic is indicated by horizontal bars. The calculations included s, p, and d orbitals but not the Madelung correction Eq. (11).

cupied d band drops relative to the Fermi level as the atomic number increases.

5.3. The alkaline earth metals

The calculated structural-energy differences for the alkaline earth metals under pressure are shown in Fig. 12. In the figure the metals are ordered according to their calculated d occupation number at equilibrium and we have included the two divalent rare earths Eu and Yb, but excluded the divalent metals Be and Mg since they do not really belong to the crystal structure sequence we shall presently be discussing. The results at zero pressure for Be and Mg may, however, be found in the preliminary account (Skriver 1982) of the present work.

According to Fig. 12, Ca, Yb, and Sr at low temperature and pressure should form in the fcc structure while Eu, Ra, and Ba should be bcc.

These predictions are in agreement with experiments (Donohue 1975, Young 1975) except for Yb which at low temperature takes up the hcp structure (Bucher et al. 1970). However, at a slightly expanded volume the hcp phase is calculated to be the stable phase, and hence one may not have to appeal to zero-point motion to explain the anomalous low-temperature hcp phase in Yb. Previous pseudopotential calculations (Animalu 1967) have explained the bcc structure in Ba and the pressure-(and temperature-) induced fcc→bcc transition in Sr, but gave an incorrect (bcc) zero-pressure crystal structure in Ca. Later pseudopotential results (Moriarty 1973) indicated that the stable structure at ordinary pressure should be the fcc structure for all the alkaline earths. Hence, it is still a challenge to pseudopotential theory to predict the crystal structures of the alkaline earth metals as a function of both atomic number and pressure.

There is a strong correlation between the calculated d occupation number and the calculated crystal structure as may be seen in Fig. 13. According to this the heavy alkaline earth metals should be part of the same hcp→fcc→bcc→hcp sequence. At zero pressure each individual metal

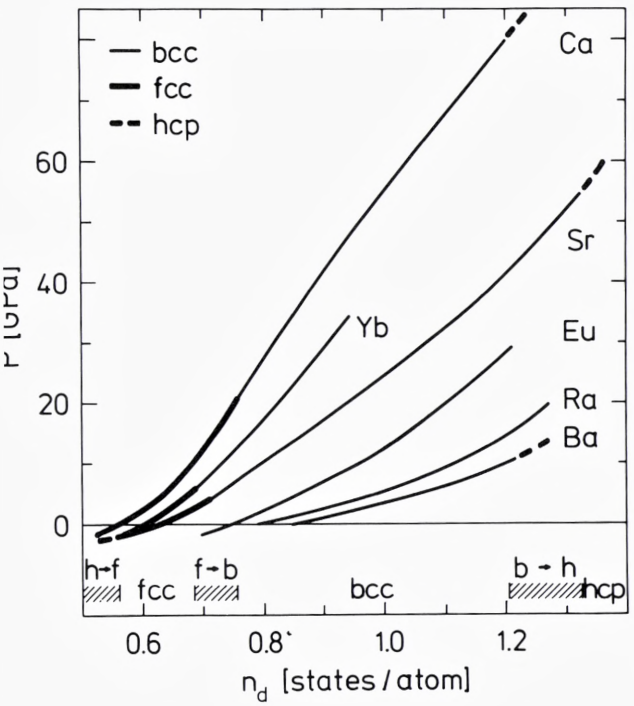

Fig. 13. Calculated crystal structures for the alkaline earth metals as functions of the LMTO pressure and d occupation number.

may be characterized as being at different stages on the continuous s-to-d transition, i.e. by their d occupation number, and the structural phase transitions are then driven by the pressure-induced lowering of the d band with respect to the s band. The correlation is, however, not perfect and the calculated crystal-structure changes occur over a narrow range of d occupation numbers.

Experimentally (Jayaraman et al. 1963a, b, Jayaraman 1964, Olijnyk and Holzapfel 1984) one observes at room temperature the fcc→bcc part of the above sequence but the bcc→hcp transition is found only in Ba whereas the lighter alkaline earth metals transform into more complex high-pressure phases (Olijnyk and Holzapfel 1984) not considered here. The critical pressures for the fcc→bcc transition in Ca, Sr, and Yb plus the bcc→hcp transition in Ba are calculated to be 21, 3.8, 5.5, and 10 [GPa], respectively (cf. Fig. 13). At room temperature Olijnyk and Holzapfel (1984) find experimentally 19.7 [GPa] for the transition in Ca while a low-temperature extrapolation of the high pressure crystallographic measurements by Jayaraman et al. (1983a, b) and Jayaraman (1964) gives 4, 5, and 5 [GPa] for the latter three transitions. In view of the fact that no adjustable parameters have been used to construct Fig. 13, the agreement with the calculated critical pressures may be considered satisfactory.

The band structure calculations show in agreement with the high-pressure resistivity data (Stager and Drickamer 1963a, b, Souers and Jura 1963, McWhan et al. 1963) that Ca, Sr, and Yb in the fcc phase should undergo a metal-semimetal-metal transition under pressure as described in detail for Ca by, for instance, Jan and Skriver (1981). Recently, Dunn and Bundy (1981) re-measured Ca and found the pressure range of the semimetallic phase to be much narrower than that found in earlier measurements (Stager and Drickamer 1963a) or predicted by band theory (McCaffrey et al. 1973, Mickish et al. 1974, Jan and Skriver 1981). Jan and Skriver (1981), for instance, predicted that fcc Ca should be semimetallic from 4 to 29 [GPa]. In the present extension of those calculations it is seen in Fig. 12 that before Ca reaches 29 [GPa] it is expected to transform into the bcc phase whereby the semimetallic behaviou will be terminated already at 21 [GPa]. This termination of the semimetallic phase at approximately 20 [GPa] is in agreement with both resistivity (Dunn and Bundy 1981) and crystallographic (Olijnyk and Holzapfel 1984) measurements. However, the critical pressure of 4 [GPa] for the onset of the semimetallic behaviour is still too low compared to that obtained from the resistivity data of Dunn and Bundy (1981), and this

discrepancy must be due to a failure of local-density theory of the kind mentioned by Jan og Skriver (1981).

In recent high-pressure measurements (Holzapfel et al. 1979, Takemura and Syassen 1985) both Eu and Yb are found to transform from the bcc to the hcp phase in seeming agreement with the systematics exhibited in Fig. 13. However, since Yb (Syassen et al. 1982) and presumably also Eu (Johansson and Rosengren 1975, Rosengren and Johansson 1976) change valence under pressure their high-pressure hcp phase is more appropriately thought of as belonging to the rare earth sequence, see Fig. 1, whereby it follows that Eu and Yb at very high pressures should exhibit the well-known hcp→Sm-type→dhcp→fcc transitions.

5.4. The transition metals

The calculated structural energy differences for the 3d, 4d, and 5d transition metals are shown in Fig. 14 and, as a comparison will show, the predicted crystal structures of all the metals included in this figure, neglecting the three ferromagnetic 3d metals, agree with the experimentally observed crystal structures, Fig. 1, except for the case of Au where the bcc structure is calculated to be marginally more stable than fcc. Hence, it follows that by including complete, i.e. fully hybridized, band structures for each individual metal but still retaining the force theorem one has cured most of the problems connected with the simple canonical picture discussed in Sect. 1.2 and exemplified in Fig. 7. Furthermore, one should note that the correlation between crystal structure and d occupation which the canonical description predicts remains valid also for the complete calculations.

The results in Fig. 14 are very similar to those obtained by Pettifor (1970, 1972, 1977) for the 3d metals and by Williams (quoted by Miedema and Niessen 1983) for the 4d metals. However, in spite of the agreement of the theoretical calculations to within 25% and the correct prediction by the theory of the crystal structures of 27 metals, the calculated structural energy differences are found to be as much as a factor of 3-5 larger than the enthalpy differences obtained from the study of binary phase diagrams (Miedema and Niessen 1983), Fig. 15. At present the cause of this discrepancy is not known. The most likely candidates are either neglect of non-spherical terms in the charge density or a genuine failure of the local density approximation. The force theorem itself does not seem to be the cause of the discrepancy since Williams as quoted by Miedema and Niessen (1983) obtains results similar to ours by subtraction of total energy calculations. Finally, the »experimental« results de-

Fig. 14. Structural energy differences for the 3d, 4d, and 5d transition metals calculated at the experimentally observed equilibrium volume and plotted as functions of the d occupation numbers. The calculations included s, p, and d orbitals but not the Madelung correction Eq. (11).

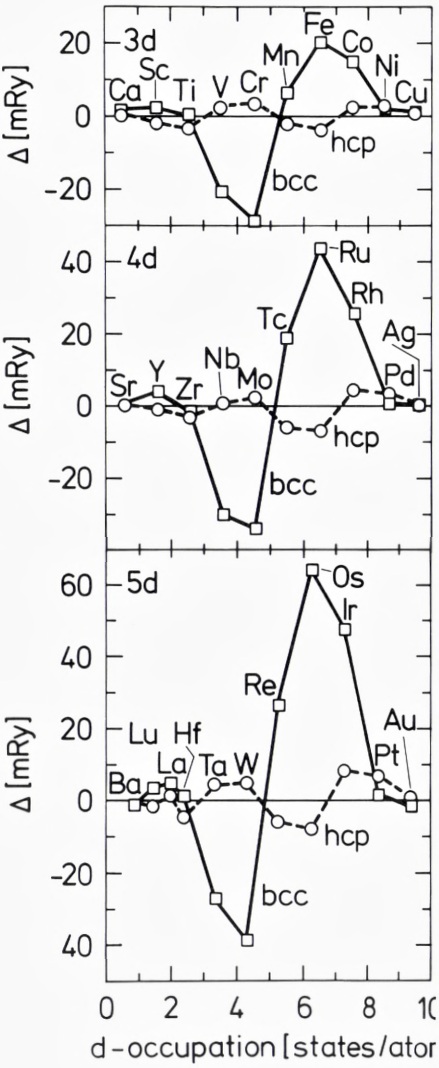

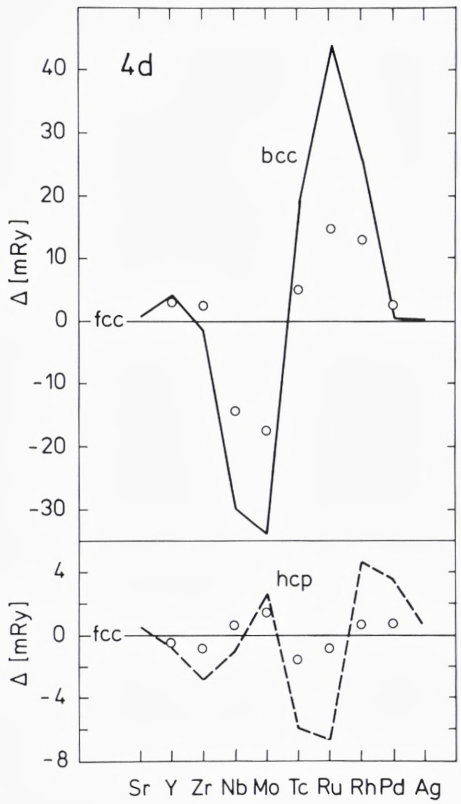

Fig. 15. The calculated bcc-fcc and hcp-fcc structural energy differences (solid and broken lines) for the 4d metals compared with the enthalpy differences derived from phase diagrams (Miedema and Niessen 1983), open circles.

rived by Miedema and Niessen (1983) are certainly model dependent and may therefore have large error bars.

5.5. The lanthanide metals

The calculated structural-energy differences for the two lanthanide metals La and Lu which bracket the lanthanide series are shown in Fig. 16. To compare directly with the canonical results, Fig. 6, the energy differences have been brought onto the canonical scale and plotted as functions of the calculated d occupation number. The results in Fig. 16 are qualitatively similar to the canonical results but the energy differences are generally smaller by approximately a factor of 2, judged by, for instance, the minimum in the Sm-type curve, than their canonical counterparts. Furthermore, the lanthanide sequence has been shifted to lower d occupation numbers whereby the problems connected with the canonical description in the d occupation range above 1.6 have been removed. Hence, Ti, Zr, and Hf are no longer part of the lanthanide sequence and are instead correctly predicted to form in the hcp structure, Fig. 14.

In an account of the cohesive properties of the lanthanides Skriver (1983) found that the d occupation numbers calculated at the experimentally observed equilibrium volume decreased approximately linearly

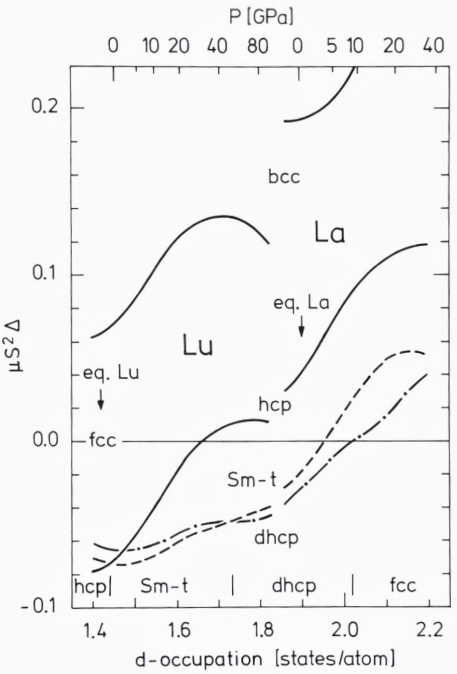

Fig. 16. Structural energy differences for La and Lu calculated as functions of pressure P and plotted versus d occupation number n_d. The calculations included s, p, d, and f orbitals, 4f for La and 5f for Lu, but not the Madelung correction Eq. (11).

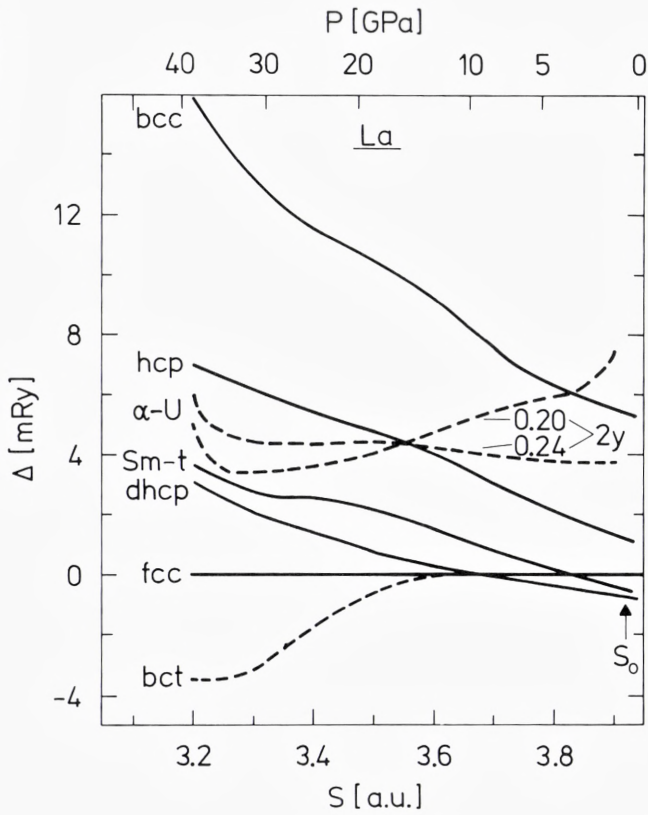

Fig. 17. Structural energy differences for La calculated as functions of pressure P and plotted versus atomic radius. The equilibrium radius S_o = 3.92 [a.u.].

with atomic number between La and Lu. Hence, Fig. 16 may be used to estimate the equilibrium crystal structures of the lanthanide metals, excluding Ce because of its γ-α transition, and the two divalent metals Eu and Yb. In agreement with the generalized phase diagram (Johansson and Rosengren 1975) we find that La, Pr, Nd, and Pm should form in the dhcp structure while Sm should be Sm-type. However, the heavy lanthanides are incorrectly estimated to form in the Sm-type structure. The immediate reason for this failure seems to be that the stability of the hcp structure at a given d occupation is calculated to be too low compared with dhcp and Sm-type but the deeper cause is not known at present. As a result, the Sm-type structure extends over too wide a d occupation range.

Fig. 16 may also be used to predict the behaviour of La and Lu under pressure. We find that Lu should transform from hcp to the Sm-type structure at – 2 [GPa] and into the dhcp structure at 35 [GPa]. Because of a 2% error in the calculated equilibrium radius and because of the failure

mentioned above, the first estimate is in error by 25 [GPa], the experimental critical pressure being 23 [GPa] (Liu 1975). The second transition has not yet been observed.

Under pressure La is predicted to transform from dhcp to the fcc structure at 8 [GPa], Fig. 17, which compares favourably with the experimental room-temperature transition pressure of 2.5 [GPa] (Piermarini 1964). The distorted fcc phase discovered by Grosshans et al. (1982) has not been considered, but we shall return to the high-pressure properties of La in the following section.

5.6. Cerium metal under pressure

The behaviour of Ce under pressure has been a subject of long-standing and some controversy, primarily because of the unusual isostructural

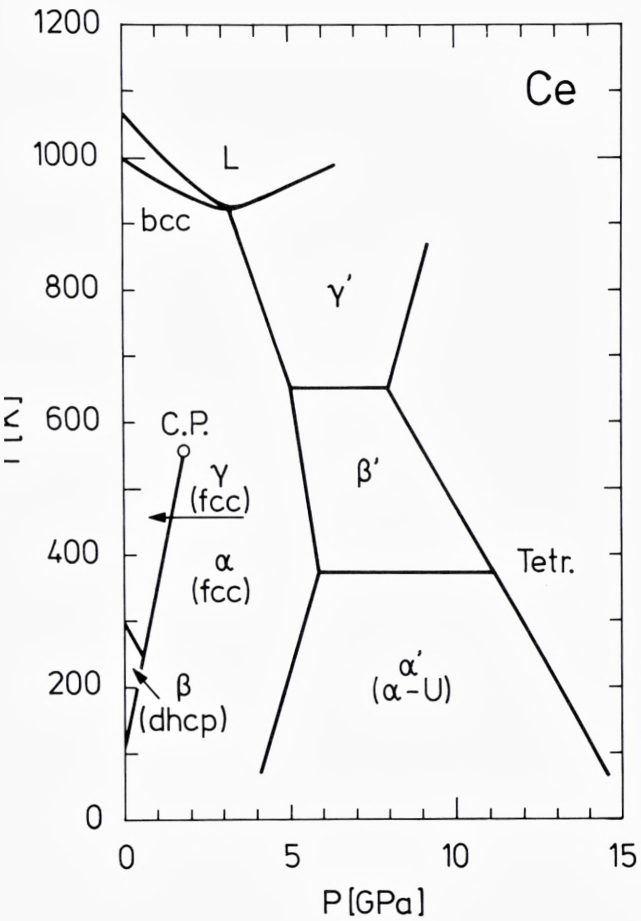

Fig. 18. Phase diagram for Ce compiled from Khvostantsev et al. (1983).

$\gamma \rightarrow \alpha$ transition. Here we shall be concerned with the fcc→α-U→tetragonal crystal-structure sequence exhibited by metallic Ce at low temperature in the pressure range up to 20 [GPa] (see Fig. 18). In the calculations we shall treat the s, p, d, and the 4f electrons on the same footing, i.e. as band electrons. Hence, we favour the picture of the $\gamma \rightarrow \alpha$ transition suggested by Gustafson et al. (1969) and elaborated by Johansson (1974) according to which pressure induces a Mott transition within the 4f shell such that the 4f electron goes from a localized state in γ-Ce to a delocalized, i.e. band state, in α-Ce.

According to the Mott-transition picture Ce metal at pressures above the $\gamma \rightarrow \alpha$ transition is different from the other lanthanides (and indeed from all the other metals we have considered so far) in that it has a fourth conduction electron residing in the 4f band. It is this occupation of the 4f band which is expected to be responsible for the stability of the α-U structure found experimentally above 5.6 [GPa] (Ellinger and Zachariasen 1974) and perhaps for the tetragonal phase found above 12.1 [GPa] (Endo et al. 1977). To shed light on this question we shall now present a series of calculations of structural stabilities for Ce under pressure, and compare the results with those obtained for La where the 4f band is essentially empty.

The orthorombic α-U structure may be viewed as distorted fcc, where some of the face-centered atoms have been moved away from their positions as described by the parameter 2y, see Fig. 19. If $2y = 0.5a$ and $a = b = c$ one has the usual fcc unit cell. In the case of Ce the Madelung contribution to the structural energy favours a 2y of approximately 0.3 (see top panel of Fig. 19) but the one-electron contribution moves the minimum in the energy difference to $2y = 0.21$ which is the 2y value found experimentally in U (Donohue 1975). Under pressure the minimum is seen to move to slightly lower 2y values and eventually the α-U structure becomes more stable than the fcc.

From fig. 19 it is expected that Ce will exhibit an fcc→α-U phase transition at a pressure which is calculated to be 11.7 [GPa]. The experimental transition pressure is 5.6 [GPa] (Ellinger and Zachariasen 1974), and the discrepancy may be attributed to the fact that the atomic sphere approximation is less suited for open crystal structures such as the α-U structure. As may be seen in Fig. 19 the Madelung correction, which we could neglect for the close-packed crystal structures of the alkaline earth and transition metals is now of the same order of magnitude as the one-electron contribution. Hence, inadequacies in the Madelung approximation of the electrostatic contribution to the structural energy are magni-

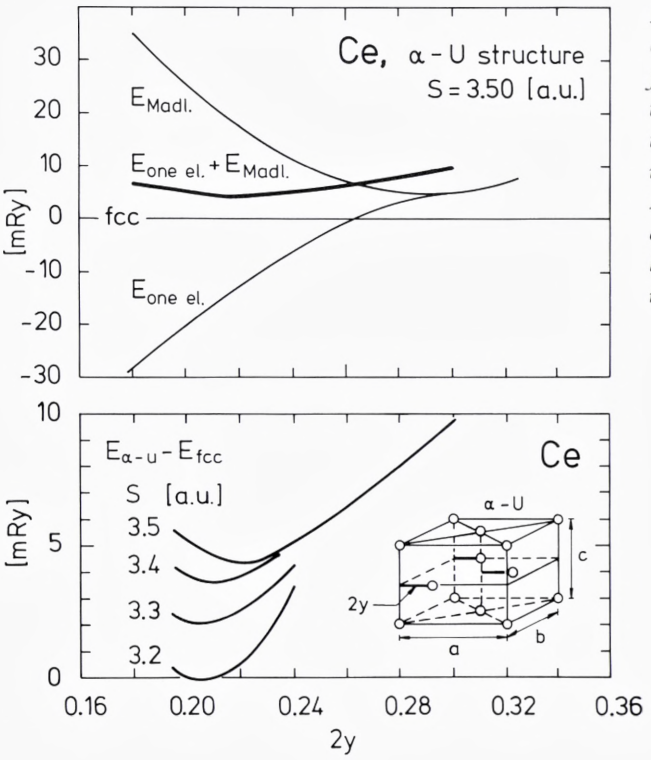

Fig. 19. Energy of Ce in the α-U structure relative to the fcc phase calculated as a function of the positional parameter 2y (see insert) and atomic radius S. The individual Madelung and one-electron contributions for one particular radius are shown in the upper panel.

fied and lead to errors in the estimate of the stability of the α-U structure. A similar problem was recently encountered in the case of the open Cs IV structure in Cs metal (McMahan 1984).

If we compare the structural energy-differences for Ce and La (Figs. 17, 19) under pressure we find that while the α-U structure eventually becomes more stable than fcc in Ce it does not do so in La. Since the 4f band is essentially unoccupied in La, whereas Ce has approximately one 4f band electron, the notion that f-band states are responsible for the stability of distorted crystal structures such as the α-U structure is strongly supported by the present calculations. It follows that the α-U structure would not become stable in Ce under pressure unless the 4f electrons were delocalized, i.e. band like, and therefore any adequate description of the α and α' phases in Ce must treat the 4f states on the same footing as the s, p, and d states. In short, Ce is a 4f band metal.

The high-pressure tetragonal structure (Endo et al. 1977) of Ce may be regarded as a distorted fcc structure in which the unit cell has been elongated along the c axis such that the c/a ratio in a body-centred

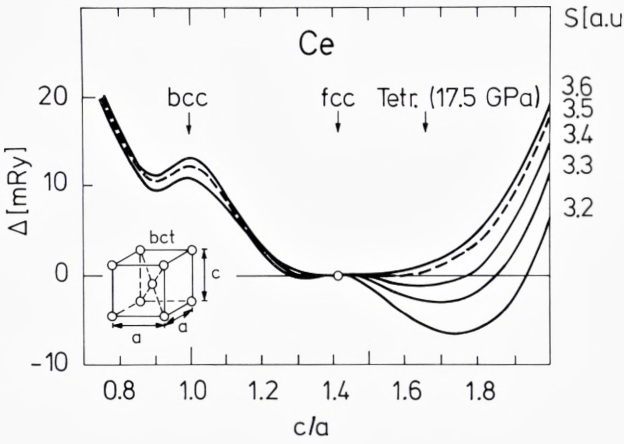

Fig. 20. Energy of Ce in the body-centred tetragonal (bct) structure relative to the fcc phase calculated as a function of the c/a ratio and atomic radius (the pressures can be inferred from Fig. 21). The insert shows the bct structure.

tetragonal (bct) description is approximately 1.7, see Fig. 20. In the same description bcc and fcc correspond to c/a equal to 1 and $\sqrt{2}$, respectively. According to the structural energy differences in Fig. 20 Ce should as a function of pressure start out in the fcc structure and then transform into a bct structure with a c/a ratio which increases with pressure. In this case the 4f states do not seem to be responsible for the pressure-induced transition, since the same bct structure is also calculated to be the stable high-pressure phase of La, Fig. 17.

In Fig. 21 we have collected the calculated structural energy differences for Ce under pressure. Owing to the less accurate description of open structures discussed above, the α-U structure is seen not to be the stable phase in the pressure range considered, and instead Ce would be expected to go directly from the fcc into the bct phase. However, if we move the α-U curve down by 4.5 [mRy] which is 20% of the Madelung correction (see Fig. 19) we obtain agreement with experiment (Ellinger and Zachariasen 1974, Endo et al. 1977) in the sense that Ce is now expected to exhibit the crystal structure sequence fcc→α-U→tetragonal.

5.7. The light actinides

The calculated structural energy differences for the light actinides Th-Pu are shown in Fig. 22, from which we deduce the most stable close-packed structure to be fcc in Th and Pa and bcc in U, Np, and Pu. This indicates that although these structures are not the stable low-temperature structures in Pa-Pu, they are at least close in energy to the distorted structures observed experimentally and may therefore be realized at elevated temperatures. Experimentally one finds the fcc structure to be

stable in Th up to 1670 [K] (Donohue 1975, Young 1975), and there are indications that Pa has a high temperature fcc phase (Donohue 1975). Furthermore, neither U nor Np has a high temperature fcc phase but instead they become bcc before melting. Pu has a high temperature fcc (δ) phase but since this phase becomes unstable at a pressure of only 0.1 [GPa] it is most probably associated with a localization of the 5f electrons, and the relevant high temperature phase in the present context is then the bcc (ε) phase. Thus, experimentally the most stable close-packed structure appears to be fcc in Th and Pa, and bcc in U, Np, and Pu, in agreement with the findings in Fig. 22.

The low-temperature tetragonal structure (α) in Pa may be viewed (Zachariasen 1952) as a distorted bcc structure in which the unit cell has been compressed along the c axis such that the c/a ratio is approximately 0.82, see Fig. 23. According to Fig. 23 the Madelung contribution

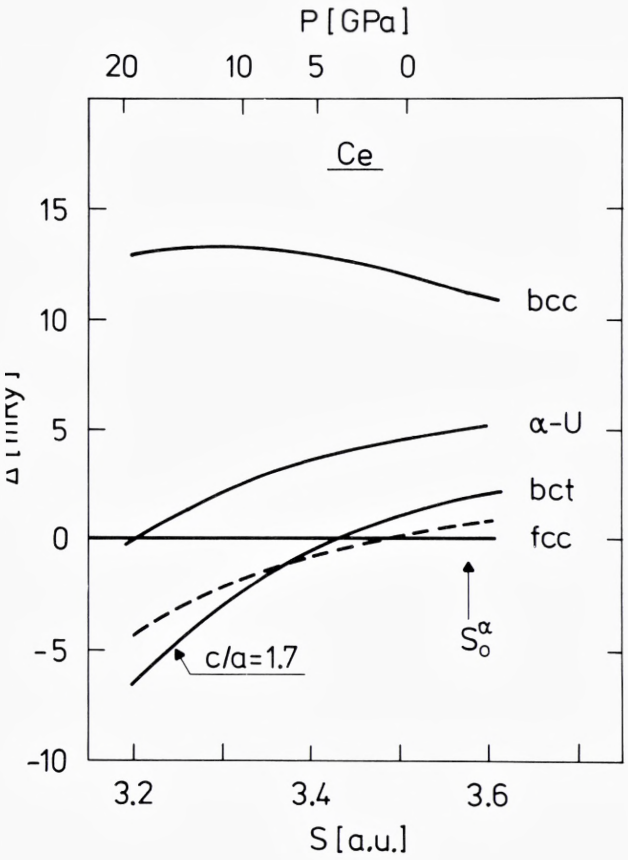

Fig. 21. Structural energy differences for Ce calculated as a function of pressure P and plotted versus atomic radius. S_o^α indicates the experimentally observed equilibrium radius of Ce in the α phase. The calculations included s, p, d, and f orbitals and the Madelung correction Eq. (11).

favours bct structures with c/a in the range from 0.95 to 1.50, whereas structures with c/a outside this range rapidly become extremely unstable. In contrast, the one-electron contribution tends to favour c/a outside the central range, and as a result the energy difference curve for Th has one minimum at c/a = $\sqrt{2}$, corresponding to fcc, in agreement with experiment, while that of Pa exhibits three minima, one of which is close to the c/a observed experimentally in the α phase.

As in the case of the α-U structure in Ce, we are again experiencing problems stemming from the atomic sphere approximation and in particular the Madelung correction, which leads to slightly incorrect estimates of the structural energy differences for open crystal structures. Thus, in the case of Pa the most stable structure is calculated to be bct with c/a = 1.6, which incidentally is the high-pressure phase of Ce, whereas the minimum which corresponds to the experimental α structure lies 1.3 mRy above the absolute minimum and is shifted to a c/a of 0.92. However, in view of the rapidly changing Madelung correction in the range below c/a = 0.95, it is not unlikely that a better calculation of the electrostatic contribution to the structural energy differences may correct both errors.

Since the 5f band is unoccupied in Th while Pa has approximately one 5f electron it follows from Fig. 23 that the 5f states are responsible for the stability of the tetragonal α phase in Pa. Thus, the situation here is very

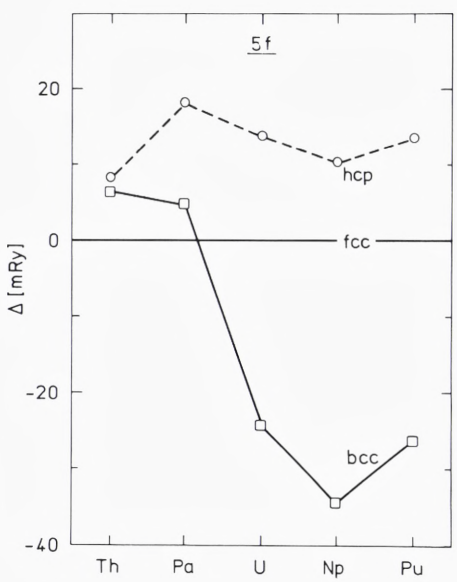

Fig. 22. Calculated structural energy differences for the light actinides plotted versus atomic number. The calculations included s, p, d, and f orbitals but not the Madelung correction Eq. (11).

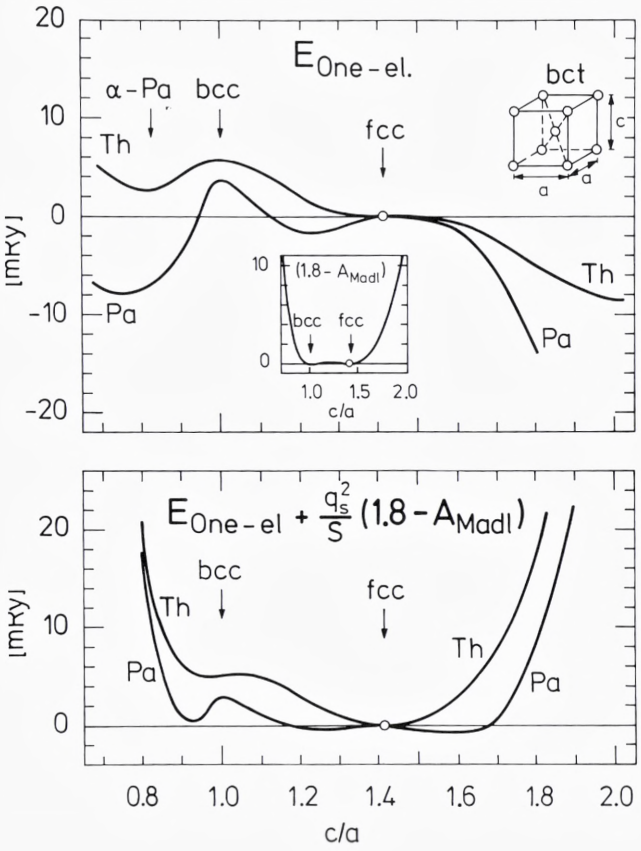

Fig. 23. Energy of Th and Pa in the bct structure relative to the fcc phase calculated as a function of the c/a ratio. The upper panel shows the one-electron contributions, the insert shows the shape of the Madelung correction, and the lower panel shows the total energy differences.

similar to that found earlier in Ce where the presence of one 4f electron stabilized the high pressure α-U structure, and again we take this to mean that the 5f states in the light actinides are itinerant, i.e. band-like, and give rise to distorted crystal structures.

6. Conclusion

We have studied the stability of the crystal structures of some 40 elemental metals within a one-electron approach. The effective one-electron equations have been solved self-consistently by means of the LMTO method and the structural energy differences calculated by means of Andersen's force theorem. This approach has the advantage of treating s, p, d, and f states on the same footing, thus leading to a conceptually

consistent description of trends throughout the periodic table. However, the present implementation of the method is only accurate for close-packed crystal structures, and for that reason we exclude in our study open structures such as CsIV and the more exotic structures found in the actinide series. On the other hand, this shortcoming is not fundamental and will undoubtedly be remedied in the near future.

We find that the theory correctly predicts the crystal structures observed experimentally at low temperature and atmospheric pressure in 35 out of the 42 cases studied. In those few instances where the theory fails we find that the correct crystal structure is only marginally less stable than the calculated structure – this is the case for Na, Au, Yb, and Pa – or the metal is magnetic at low temperature, as in Mn, Fe, and Co. For the light actinides U, Np, and Pu we have not considered the experimentally most stable crystal structures but only the most stable close-packed structures and find the predictions of the theory to be in qualitative agreement with the known phase diagrams.

In a comparison between the calculated structural energy differences for the 4d transition metals and the enthalpy differences derived from studies of phase diagrams we find that, although the crystal structures are correctly predicted by the theory, the theoretical energy differences are up to a factor of 5 larger than their »experimental« counterparts. The reasons for this discrepancy may lie in the local-density approximation or in the neglect of the non-spherical part of the charge distribution. Furthermore, the derived enthalpy differences are certainly model dependent and may change as the model is improved.

In addition to the equilibrium properties we have studied the crystal structures of the alkali, the alkaline earth and some rare earth metals under pressure. We find that the heavy alkalis K, Rb, and Cs should be part of the crystal structure sequence bcc→hcp→fcc where the intermediate hcp phase may be suppressed at room temperature, and explain the experimentally observed bcc→fcc transition in terms of the pressure-induced descent of a zone-boundary energy gap which exists in the fcc band structure but has no counterpart in the bcc case. For the alkaline earth and rare earth metals we find crystal structure sequences which correlate with the calculated d-occupation numbers and which are in agreement with experimental high-pressure observations if we neglect some complex structures found in Ca and Sr.

Finally, we have studied the high-pressure crystal structure sequence fcc→α-U→tet for La and Ce and find that under compression the α-U structure becomes more stable than fcc in Ce, but not in La. This indi-

cates that the presence of itinerant 4f states is responsible for the fcc→α-U transition observed experimentally in Ce. In both La and Ce the calculations predict a tetragonal high-pressure phase. This phase is seen experimentally in Ce but not in La where one instead observes a distorted fcc structure not considered in the present work.

In conclusion, we have studied the stability of crystal structures of metals both at equilibrium and at high pressures by a one-electron approach. We find that we can account for the occurence of most of the close-packed structures observed experimentally. In the few cases where the theory is in disagreement with experiment we find that the correct crystal structure is only marginally less stable than the predicted structure. In order to describe open structures, such as α-U or CsIV, with the same accuracy as the close-packed structures one needs a more accurate approximation for the electrostatic contribution to the total energy.

ACKNOWLEDGMENTS. *The present series of calculations grew out of conversations with several people. It is thus a great pleasure to thank K. Syassen and K. Takemura for making me interested in the alkali metal problem, and B. Johansson for suggesting the Ce problem. B. Johansson and A. K. McMahan have furthermore helped clarify calculational as well as experimental problems. Part of this work was started while visiting Los Alamos Scientific Laboratory, and I wish to thank the group at the Materials Science Center for its kind hospitality. Finally, I want to express my gratitude to Knud Højgaards Fond for granting my Niels Bohr Fellowship.*

References

J. Akella, Q. Johnson, W. Thayer, and R. N. Schock, J. Less-Comm. Met. *68,* 95 (1979).

J. Akella, Q. Johnson, and R. N. Schock, Geophysical Res. *85,* 7056 (1980).

I. V. Alexandrov, C. V. Nesper, V. N. Katchinsky and J. Marenko, paper at the 20th meeting of the »European High pressure Research Group«, Stuttgart, 1982 (unpublished).

O. K. Andersen, Phys. Rev. *B12,* 3060 (1975).

O. K. Andersen and O. Jepsen, Physica *91B,* 317 (1977).

O. K. Andersen, J. Madsen, U. K. Poulsen, O. Jepsen, and J. Kollar, Physica *86-88B,* 249 (1977).

O. K. Andersen, H. L. Skriver, H. Nohl, and B. Johansson, Pure Appl. Chem. *52,* 93 (1979).

A. O. E. Animalu, Phys. Rev. *161,* 445 (1967).

J. Bardeen, J. Chem. Phys. *6,* 372 (1938).

U. von Barth and L. Hedin, J. Phys. *C5,* 1629 (1972).

B. J. Beaudry and K. A. Gschneidner, Jr., »Preparation and Basic Properties of the Rare Earth Metals« in *»Handbook on the Physics and Chemistry of Rare Earths«* ed. by K. A. Gschneidner, Jr. and L. R. Eyring (North Holland Publishing Company, Amsterdam 1978).

U. Benedict, J. R. Peterson, R. G. Haire, and C. Dufour, J. Phys. *F14,* L43 (1984).
M. Born and J. E. Mayer, Zeits. f. Physik *75,* 1 (1932).
L. Brewer: »Phase Stability in Metals and Alloys« in *»Batelle Institute Materials Science Colloquia«,* ed. by P. S. Rudman, J. Stringer, and R. I. Jaffee (McGraw-Hill, New York 1967), pp. 39-62.
E. Bucher, P. H. Schmidt, A. Jayaraman, K. Andres, J. P. Maita, K. Nassau, and P. D. Dernier, Phys. Rev. *B2,* 3911 (1970).
M. S. S. Brooks and B. Johansson, J. Phys *F13,* L197 (1983).
N. W. Dalton and R. A. Deegan, J. Phys. *C2,* 2369 (1969).
R. A. Deegan, J. Phys. *C1,* 763 (1968).
J. Donohue, »The Structures of the Elements« (John Wiley & Sons, New York 1975).
F. Ducastelle and F. Cyrot-Lackmann, J. Phys. Chem. Solids *32,* 285 (1971).
K. J. Dunn and F. P. Bundy, Phys. Rev. *B24,* 1643 (1981).
J. C. Duthie and D. G. Pettifor, Phys. Rev. Lett. *38,* 564 (1977).
F. H. Ellinger and W. H. Zachariasen, Phys. Rev. Lett. *32,* 773 (1974).
S. Endo, H. Sasaki, and T. Mitsui, J. Phys. Soc. Japan *42,* 882 (1977).
E. Esposito, A. E. Carlsson, D. D. Ling, H. Ehrenreich, and C. D. Gelatt, Jr., Phil. Mag. *A41,* 251 (1980).
J. Friedel, »Transition Metals. Electronic Structure of the d-band. Its Role in the Crystalline and Magnetic Structures« in *»The Physics of Metals 1. Electrons«* ed. by J. M. Ziman (Cambridge University Press 1969).
J. Friedel and C. M.. Sayers. J. Physique *38,* 697 (1977).
D. Glötzel and A. K. McMahan, Phys. Rev. *B20,* 3210 (1979).
W. A. Grosshans, Y. K. Vohra, and W. B. Holzapfel, Phys. Rev. Lett. *49,* 1572 (1982).
K. A. Gschneidner, »Physical Properties and Interrelations of Metallic and Semimetallic Elements« in *»Solid State Physics«* vol. *16,* ed. by H. Ehrenreich, F. Seitz, and D. Turnbull (Academic Press, New York 1964).
K. A. Gschneidner and R. M. Valletta, Acta Met. *16,* 477 (1968).
D. R. Gustafson, J. D. McNutt and L. O. Roellig, Phys. Rev. *183,* 435 (1969).
J. Hafner and V. Heine, J. Phys. *F13,* 2479 (1983) and references therein.
H. T. Hall, L. Merril, and J. D. Barrett, Science *146,* 1297 (1964).
V. Heine and D. Weaire, »Pseudopotential Theory of Cohesion and Structure« in *»Solid State Physics«* vol. *24* ed. by H. Ehrenreich, F. Seitz, and D. Turnbull (Academic press, New York 1970).
V. Heine, »Electronic Structure from the Point of View of the Local Atomic Environment« in *»Solid State Physics«* vol. *35* ed. by H. Ehrenreich, F. Seitz, and D. Turnbull (Academic Press, New York 1980).
C. H. Hodges, Acta Met. *15,* 1787 (1967).
W. B. Holzapfel, T. G. Ramesh, and K. Syassen, J. de Phys. Coll. *40,* C5-390 (1979).
J.-P. Jan and H. L. Skriver, J. Phys. *F11,* 805 (1981).
A. Jayaraman, W. Klement, Jr., and G. C. Kennedy, Phys. Rev. Lett. *10,* 387 (1963a).
A. Jayaraman, N. Klement, Jr., and G. C. Kennedy, Phys. Rev. *132,* 1620 (1963b).
A. Jayaraman, Phys. Rev. *135,* A1056 (1964).
A. Jayaraman and R. C. Sherwood, Phys. Rev., *134,* A691 (1964).
A. Jayaraman, Phys. Rev. *139,* A690 (1965).
B. Johansson, Phil. Mag. *30,* 469 (1974).
B. Johansson and A. Rosengren, Phys. Rev. *B11,* 2836 (1975).

B. Johansson, »Structural and elastic properties of the f elements« in *»Rare Earths and Actinides, 1977«* ed. by W. D. Corner and B. K. Tanner (IOP, Bristol 1978), p. 39 (Inst. Phys. Conf. Ser. No. *37*).
H. Jones, Prog. Phys. Soc. *49,* 250 (1937).
L. Kaufman and H. Bernstein: »Computer Calculations of Phase Diagrams« (Academic Press, New York 1970).
L. G. Khvostantsev and N. A. Nikolaev, Phys. Stat. Sol. (a) 77, 161 (1983).
C. C. Koch, J. Less-Comm. Met. *22,* 149 (1970).
W. Kohn and L. J. Sham, Phys. Rev. *140A,* 1135 (1965).
L.-G. Liu, W. A. Bassett, and M. S. Liu, Science *180,* 298 (1973).
L.-G. Liu, J. Phys. Chem. Solids *36,* 31 (1975).
J. W. McCaffrey, J. R. Anderson, and D. A. Papaconstantopoulos, Phys. Rev. *B7,* 674 (1973).
A. R. Machintosh and O. K. Andersen, »The electronic structure of transition metals« in *»Electrons at the Fermi surface«* ed. by M. Springford (Cambridge University Press, Cambridge 1980).
A. K. McMahan and J. A. Moriarty, Phys. Rev. *B27,* 3235 (1983).
A. K. McMahan, Phys. Rev. *B29,* 5982 (1984).
D. B. McWhan and A. L. Stevens, Phys. Rev. *139,* A682 (1965).
D. B. McWhan and A. L. Stevens, Phys. Rev. *154,* 438 (1967).
D. B. McWhan, T. M. Rice, and P. H. Schmidt, Phys. Rev. *177,* 1063 (1969).
D. J. Michish, A. B. Kunz, and S. T. Pantalides, Phys. rev. *B10,* 1369 (1974).
A. R. Miedema and A. K. Niessen, CALPHAD 7, 27 (1983).
J. A. Moriarty, Phys. Rev. *B8,* 1338 (1973).
J. A. Moriarty, Phys. Rev. *B26,* 1754 (1982).
J. A. Moriarty and A. K. McMahan, Phys. Rev. Lett. *48,* 809 (1982).
N. F. Mott and H. Jones, »The Theory of the Properties of Metals and Alloys« (Oxford Univ. Press, London 1936).
A. Nakaue, J. Less-Comm. Met. *60,* 47 (1978).
R. M. Nieminen and C. H. Hodges, J. Phys. *F6,* 573 (1976).
H. Olijnyk and W. B. Holzapfel, Phys. Lett. *99A,* 381 (1983).
H. Olijnyk abd W. B. Holzapfel, Phys. Lett. *100A,* 191 (1984).
B. Olinger and J. W. Shaner, Science *219,* 1071 (1983).
D. G. Pettifor, J. Phys. *C3,* 367 (1970).
D. G. Pettifor: »Theory of the Crystal Structures of Transition Metals at Absolute Zero« in *»Metallurgical Chemistry«* ed. by O. Kubashewski (HMSO, London 1972).
D. G. Pettifor, Commun. Phys. *1,* 141 (1976).
D. G. Pettifor, CALPHAD *1,* 305 (1977).
G. J. Piermarini and C. E. Weir, Science *144,* 69 (1964).
R. B. Roof, R. G. Haire, D. Schiferl, L. A. Schwalbe, E. A. Kmetko, and J. L. Smith, Science *207,* 1353 (1980).
R. B. Roof, Z. für Krist. *158,* 307 (1982).
A. Rosengren and B. Johansson, Phys. Rev. *B13,* 1468 (1976).
H. L. Skriver, Phys. Rev. Lett. *49,* 1768 (1982).
H. L. Skriver, »Electronic Structure and Cohesion in The Rare Earth Metals« in *»Systematics and the Properties of the Lanthanides«* ed. S. P. Sinha (D. Reidel Publishing Company, Dordrect 1983).

H. L. Skriver, »The LMTO Method« (Springer-Verlag, Berlin 1984).
P. C. Souers and G. Jura, Science *140,* 481 (1963).
R. A. Stager and H. G. Drickamer, Phys. Rev. *131,* 2524 (1963).
R. A. Stager and H. G. Drickamer, Science *139,* 1284 (1963).
D. R. Stephens, H. D. Stromberg, and E. M. Lilley, J. Phys. Chem. Solids *29,* 815 (1968).
K. Syassen, G. Wortmann, J. Feldhaus, K. H. Frank, and G. Kaindl, Phys. Rev. *B26,* 4745 (1982).
K. Takemura, S. Minomura, and O. Shimomura, »Structure of Cesium and Iodine under Pressure« in *»Physics of Solids under High Pressure«* ed. by J. S. Schilling and R. N. Shelton (North-Holland, Amsterdam 1981).
K. Takemura and K. Syassen, Solid State Commun. *44,* 1161 (1982).
K. Takemura, S. Minomura, and O. Shimomura, phys. Rev. Lett. *49,* 1772 (1982).
K. Takemura and K. Syassen, Phys. Rev. *B28,* 1193 (1983).
K. Takemura and K. Syassen, J. Phys. F (1985, in print).
A. R. Williams, unpublished, and quoted by Miedema and Niessen (1983).
Y. K. Vohra, H. Olijnyk, W. A. Grosshans, and W. B. Holzapfel, Phys. Rev. Lett. *47,* 1065 (1981).
D. A. Young, »Phase Diagrams of the Elements«, Lawrence Livermore Laboratory Report UCRL-51902 (1975, unpublished).
D. A. Young and M. Ross, Phys. Rev. *B29,* 682 (1984).
W. H. Zachariasen, Acta Cryst. *5,* 19 (1952).
A. Zunger and M. L. Cohen, Phys. Rev. *B18,* 5449 (1978); *B20,* 4082 (1979).